CHAPTER 2

Synthesis, Characterization and Antitumor Activity of Methotrexate-loaded Linear Poly(D,L-lactide)-*b*-Poly(*N*-vinylpyrrolidone) Amphiphilic Block Copolymers

2.1 Introduction

Amphiphilic block copolymers have drawn wide range of interest from all the aspects of material science owing to their self-assembly property. Amphiphic block copolymer can easily generate nanosized micelle (in water) or, reverse micelles (in oil) which found excellent applications as nanocarrier for targeted drug delivery, [Kedar *et al*. (2010)] coatings, [Lee *et al*. (2006), Chen *et al*. (2009), Shin *et al*. (2009), Callewaert *et al*. (2005)] nanoparticle synthesis, [Spatz *et al*. (1996), Liu *et al*. (2010), Sakai *et al*. (2005)] colloidal stabilization, [Perelstein *et al.* (2010), Bulychev *et al*. (2004), Sakai *et al*. (2004)] and as compatiblizer [Aryal *et al*. (2009), Signori *et al*. (2005), Hu *et al*.(2009] for polymer blends. The tunable synthesis of well-defined amphiphilic block copolymers for various applications through controlled polymerization root has drawn immense interest among the researchers. [Ouchi *et al*. (2009), Yamago *et al*. (2009)] At the interface of material and biomedical science, tunable and controlled synthesis of biocompatible and biodegradable amphiphilic block copolymers is under frantic development because of its great potential for pharmaceutical and biomedical applications. Recently, controlled synthesis of well-defined amphiphilic diblock copolymers of ε-caprolactone (CL) and *N*-vinylpyrrolidone (NVP) by combining the controlled ROP of CL and the controlled xanthate-mediated RAFT polymerization of NVP has been reported from our group. [Mishra *et al*. (2011)] In a similar way, amphiphilic block copolymers containing a biocompatible as well as biodegradable hydrophobic poly(D,L-lactide) (PDLLA) segment [Garrec *et al.*(2004), Gaucher *et al*. (2007), Rvenelle *et al*. (2008)] and a hydrophilic and biocompatible poly(*N*-vinylpyrrolidone) (PNVP) segment, having low toxicity, complexation capability, cryo-protectivity, lypo-protectivity and antibiofouling properties, will be very interesting for

biomedical applications. [Coessens *et al*. (2001), Wan *et al*. (2005), Bilalis *et al*. (2006)] Polymerization of D,L-lactide (DLLA) is generally carried out using ring-opening polymerization (ROP) technique. On the other hand, NVP can only be polymerized by radical polymerization since its amide keto group is not conjugated with the vinyl group. Different controlled/ living radical polymerization methods have successfully been developed for the controlled synthesis of its homopolymer and block copolymers. [Yamago *et al*. (2004), Ray *et al*. (2006), Yusa *et al* (2007), Yamago *et al*. (2007), Lu *et al*.(2007), Pound *et al*.(2008)] Reports of the synthesis of PNVP-*b*-PDLLA block copolymer are very few in the literature. Benahmed *et al.* (2001) have reported first the synthesis, characterization and self-assembly properties of PNVP-*b*-PDLLA block copolymers prepared by conventional radical polymerization of NVP using 2-isopropoxy ethanol initiator followed by conventional anionic ring-opening polymerization. Later, Luo *et al*. (2004) have reported the synthesis, characterization and self-assembly properties of PNVP-*b*-PDLLA block copolymer prepared through the combination of conventional radical polymerization of NVP in the presence of 2-mercaptoethanol chain transfer agent, and the ROP of DLLA using anionic ring-opening polymerization. Recently, Xiong *et al*. (2009) have reported the synthesis, characterization, and degradation of PDLLA-*b*-PNVP-*b*-PDLLA triblock copolymer prepared through the ROP of DLLA using dihydroxy-terminated PNVP as macro-initiator and dibutyl tin dilaurate (DBTDL) as catalyst. Here in, I report the controlled synthesis of well-defined amphiphilic block copolymers of DLLA and NVP *via* the combination of the controlled ROP of DLLA and the controlled metal-free xanthate-mediated RAFT polymerization of NVP [**Scheme 2.1**]. Firstly, PDLLA with –OH end-group (PDLLA-OH) is synthesized using ROP method. Then, the –OH end-group is

converted to the corresponding –Br end group (PDLLA-Br) through a reaction with 2-bromopropionyl bromide. This –Br end-group is then converted to *O*-ethyl xanthate end group (PDLLA-X) through an ionic substitution reaction with potassium *O*-ethyl xanthate. Finally, the controlled RAFT polymerization of NVP is performed to synthesize well-defined amphiphilic PDLLA-*b*-PNVP block copolymers using the macro chain transfer agent PDLLA-X. The polymers have been characterized by ^{1}H NMR spectroscopy and gel permeation chromatographic (GPC) techniques. Further, the self-assembly behavior of the resultant amphiphilic block copolymers is studied using ^{1}H NMR spectroscopy, fluorescence spectroscopy, transmission electron microscopy (TEM), and dynamic light scattering (DLS) techniques. Thermal property of these block copolymers is also studied by thermo gravimetric analyzer (TGA), differential thermal analyzer (DTA) and differential scanning calorimeter (DSC) techniques. Crystalline property of these block copolymers is also studied by the wide angle X-ray diffraction (WXRD) technique. In order study the efficacy of the micelles of these block copolymers as nano-carrier for drug delivery, I have loaded these micelles successfully with an anticancer hydrophobic drug methotraxate and studied the *in vitro* drug release property of the MTX-loaded PDLLA-*b*-PNVP amphiphilic block copolymers. The anti-tumor activity of these drug-loaded micelles was studied in B cell lymphomas of human and mouse. Our results suggest that MTX-loaded polymer suppress lymphoma cells *in vitro via* apoptosis better in compare to its free MTX. Moreover, these drug-loaded micelles also suppress MTX resistant lymphoma cells while free MTX remains ineffective. In addition, MTX-loaded block copolymer micelles do not cause hemolysis compared to free MTX which is toxic for RBC.

2.2 Experimental Section

2.2.1 Materials

Triethylamine (Loba Chemie, Mumbai, India, 99%), 2-bromopropionyl bromide (Fluka, Israel, >97%), stannous 2-ethylhexanoate [$Sn(Oct)_2$] (Aldrich, St Louis, USA, 99%), diethyl ether (S. D. fine, Mumbai, India), hexane (CDH, Mumbai, India), methanol (Loba Chemie, Mumbai, India, 99%), sodium hydrogen carbonate (Loba Chemie, Mumbai, India), ammonium chloride (S. D. fine, Mumbai, India), anhydrous magnesium sulfate (Loba Chemie, Mumbai, India) were used as received. Benzyl alcohol (S. D. fine, Mumbai, India, 99%) was dried over CaO and then distilled under reduced pressure. D,L-lactide (DLLA) (Aldrich, St Louis, USA, 99%) was recrystallized from ethyl acetate. *N*-Vinyl pyrrolidone (Aldrich, St Louis, USA, 99%) was dried over anhydrous magnesium sulfate and distilled under reduced pressure. 2, $2^{/}$- Azo-bis(isobutyronitrile) (AIBN) (Spectrochem, Mumbai, India, 98%) was recrystallized from methanol. Tetrahydrofuran (THF) (Loba Chemie, Mumbai, India) was dried and fractionally distilled from sodium and benzophenone. Ethanol (Saraya Distillery, India) was stirred over CaO overnight and distilled over fresh CaO. Potassium *O*-ethyl xanthate was prepared according to our previous work. [Patel *et al.* (2010)] Methotrexate (MTX) (ALKEM Laboratories Limited, Mumbai) was used as received. RPMI 1640, penicillin and streptomycin were purchased from GIBCO, Invitrogen, Carlsbad, CA and fetal bovine serum from Hyclone, Logan, UT. Annexin V Apoptosis Detection Kit (sc-4252 AK) was purchased from Santa Cruz Biotechnology, Dallas, TX, U.S.A. Other general & fine chemicals unless otherwise stated were purchased from SIGMA-ALDRICH, St. Louis, MO, USA.

2.2.2 General Methods

2.2.2.1 ^{1}H NMR Spectroscopy and Gel Permeation Chromatography

^{1}H NMR spectra were recorded on a JEOL AL300 FTNMR (300 MHz) at room temperature in $CDCl_3$ or D_2O as solvent, and were reported in parts per million (δ) from internal standard tetramethylsilane or, residual solvent peak. NVP monomer conversion (%) was determined using ^{1}H NMR spectroscopy in $CDCl_3$ by comparing the integrated peak area of the residual vinylic signals at 4.3-4.4 ppm (2H) and 7.0-7.1 ppm (1H) of the monomer with the peak area of the methylene protons adjacent to 'N' of pyrrolidone ring at 3.0-3.4 ppm (2H) of the corresponding polymer.

The number-average molecular weight (M_n) and polydispersity index (M_w/M_n) were determined by Younglin ACME 9000 Gel Permeation Chromatography in DMF at 40 ^oC with flow rate 0.5 mL/ min on two polystyrene gel columns [PL gel 5μm 10E 4 Å columns (300 × 7.5 mm)] connected in series to a Younglin ACME 9000 Gradient Pump and a Younglin ACME 9000 RI detector. The columns were calibrated against seven poly(methyl methacrylate) (PMMA) standard samples (Polymer Lab, PMMA Calibration Kit, M-M-10). The molecular weight of the PDLLA homopolymer from ^{1}H NMR spectrum in DMSO-d_6 was determined by comparing the integrated peak intensity of aliphatic methylene protons of the backbone poly(D,L-lactide) chain at ~5.2 ppm (1H) to that of the benzene protons of the polymer chain-end at ~7.35 ppm (5H). The theoretical number-average molecular weight [M_n(theor)] of the resulted PDLLA-*b*-PNVP block polymer using PDLLA-X xanthate macro chain-transfer agent was calculated using the following equation:

$$\overline{M}_n\,(\text{theor}) = \frac{[\text{NVP}]_o}{[\text{PDLLA-X}]_o} \cdot x_{\text{NVP}} \cdot M_{\text{NVP}} + M_{\text{PDLLA-X}}\,(\text{NMR})$$

where, x_{NVP} is the fraction conversion of monomer, M_{NVP} is the molecular weight of monomer, and $M_{PDLLA\text{-}X}$ (NMR) is molecular weight of the PDLLA-X xanthate macro chain-transfer agent determined from its ^{1}H NMR.

2.2.2.2 Transmission Electron Microscopy (TEM) Study

TEM images were obtained using a Techno 12, FEI, Netherland transmission electron microscope operating at an acceleration voltage of 200 kV. The TEM samples were prepared by dipping the carbon coated copper grid into the aqueous block copolymer solution (1 mg/mL) followed by the removal of extra solution with a filter paper.

2.2.2.3 Fluorescence Study

Fluorescence study was carried out on a Varian Cary Eclipse Fluorescence Spectrometer. [Mishra *et al*. (2011)] Typically, a series of aqueous PDLLA-*b*-PNVP block copolymer solutions with concentrations ranging from 5×10^{-4} to 1 mg/mL were prepared by dilution with deionized water. A pyrene stock solution in acetone was transferred to a series of vials, the acetone was evaporated under nitrogen, and the block copolymer solutions were added to the vials to get a final pyrene concentration of 6×10^{-7} M in each vial. The excitation spectra (300–360 nm) of the solutions were recorded at an emission wavelength of 394 nm using a slit width of 5 nm. The ratio of the peak intensities of the excitation spectra of pyrene at 337.07 nm ($I_{337.07}$) and 333.07 nm ($I_{333.07}$) was plotted as a function of polymer concentration. The critical micelle concentration (cmc) value was considered as the interception point of the two tangent straight lines at low concentration.

2.2.2.4 Light Scattering Study

A Brookhaven laser scattering system equipped with a BI-200SM research goniometer, a TurboCorr digital correlator (BI-9000 AT) with a maximum number of 522 channels,

and a He-Ne laser of a wavelength 632.8 nm was used to study the dynamic light scattering behavior of the block copolymers at 25 ºC. [Mishra *et al*. (2011) Paira *et al*. (2010)] Typically, dust particles from the polymer solution were removed by filtration through 0.45 μm filter prior to the experiments. The obtained intensity autocorrelation functions were analyzed by fitting to a polynomial of second order function using the Cumulant method of the BI-ISDAW software package. The average decay rate 'Γ', and scattering vector 'q', and apparent hydrodynamic radius of the micelle 'R_h' were calculated using the following equations:

$$\Gamma = q^2 \cdot D$$

where, D = translational diffusion co-efficient

$$q = 4 \pi n_s \sin\left(\frac{\theta}{2}\right)$$

where, n_s = refractive index of the solvent, θ = scattering angle

$$R_h = \frac{K_B T}{6 \pi \eta D}$$

where, k_B = Boltzmann's constant, T = temperature in Kelvin,
and η = viscosity of the solvent

Polydispersity (PD) $\mu_2/(\overline{\Gamma})^2$, where $\overline{\Gamma}$ and μ_2 are the first and second cumulants of the quadratic fitting of natural logarithm of the normalized first order intensity autocorrelation functions, provides an estimation about the size distribution width of the micelle.[Luo *et al*. (2004), Xiong *et al*. (2009)]

2.2.2.5 Thermo Gravimetric Analysis (TGA)

Thermo gravimetric analysis (TGA) was performed using Mettler TGA thermo gravimetric analyzer in the temperature range from 40 ºC to 600 ºC with a heating rate of 20 ºC /min under N_2 atmosphere.

2.2.2.6 Differential Scanning Calorimeter (DSC) Study

Differential scanning calorimeter (DSC) study was performed using Mettler 832 DSC instrument under N_2 atmosphere. The instrument was calibrated with indium before use. The samples were first heated to 150 ^oC at 20 ^oC/ min heating rate and held at this temperature for 5 min to remove the thermal history, followed by quenching to -80 ^oC. A heating rate of 10 ^oC/min was used for second heating run. Results were reported from the second heating run. The melting temperature (T_m) was taken as the temperature of the maximum of the endothermic peak.

2.2.2.7 Wide Angle X-ray Diffraction (WXRD) Study

Wide angle x-ray diffraction (WXRD) study was performed using Bruker D8 XRD instrument at an acceleration voltage of 40 kV with 40 mA current intensity using Cu tube (λ = 0.154 nm) as radiation source. XRD was measured in the range of 2θ = 10 - 40 ^{o} with the rate of 0.2 ^{o}/min.

2.2.3 Typical Synthesis of Monohydroxy-terminated Poly(D,L-lactide) ($PDLLA_{42}$-OH) (run 1, Table 1.1)

Monohydroxy-terminated poly(D,L-lactide) (PDLLA-OH) was synthesized *via* the ROP of D,L-lactide using benzyl alcohol as initiator and $Sn(Oct)_2$ as the catalyst. In a typical experiment (run 1, Table 1.1), 5 g of D,L-lactide (3.47×10^{-2} mol) was placed in a 100 mL dry Schlenk tube equipped with a magnetic bar under nitrogen atmosphere, and dried under vacuum at 80 ^oC for 4 h. After cooling, 277 μL benzyl alcohol (0.288 g, 2.67×10^{-3} mol) and 20 μL (0.025 g, 6.2×10^{-2} mmol, 0.5% w/w ratio of lactide) $Sn(Oct)_2$ were added to the flask. The reaction mixtures were purged 30 min with nitrogen. The flasks were then tightly closed, and polymerization was carried out at 150 ^oC for 16 h. The polymerization was stopped by freezing the reaction mixture with

liquid N_2. The crude product was dissolved in 10 mL of THF and precipitated from 200 mL of hexane. The precipitated polymer was collected by centrifugation. The separated polymer was purified by repeated dissolution in THF, precipitated from hexanes twice, and finally was dried under vacuum at room temperature for 24 h. Observed monomer conversion by ^{1}H NMR = 98.7%. Polymer yield = 79%.

^{1}H NMR (300 MHz, DMSO-d_6) [**Figure 2.1(A)**]: δ (ppm) = 1.27 (d, $3H_e$), 1.45 (m, $3H_d$), 4.2 (q, $1H_f$), 5.1-5.2 (m, $2H_b + 1H_c$), 7.35 (m, $5H_a$)

M_n(NMR) = 3,600 g mol^{-1}, M_n(GPC) = 4,400 g mol^{-1}, M_w/M_n = 1.55.

2.2.4. Typical Synthesis of PDLLA$_{42}$-C(O)CH(CH$_3$)Br (PDLLA$_{42}$-Br)(run 3, Table 2.1)

In a dried and nitrogen purged round-bottom flask, 3.55 g [9.95×10^{-4} mol, calculated on the basis of molecular weight (3,600 g mol^{-1}) obtained from ^{1}H NMR] of PDLLA$_{42}$-OH was dissolved in 20 mL of dry THF with 0.48 mL (3.13×10^{-3} mol) of triethylamine while stirring under nitrogen atmosphere. After that, 0.26 mL (2.48×10^{-3} mol) of 2-bromopropionyl bromide was then added drop wise to the above-mentioned reaction mixture that was cooled in an ice bath. The reaction mixture was then stirred for 72 h at room temperature. The precipitated byproduct (i.e. $Et_3N.HBr$), was removed by filtration and the filtrate was evaporated to dryness. The residue was dissolved in dichloromethane and washed thoroughly with 5% sodium bicarbonate (4 × 100 mL). The organic layer was further washed with water (4 × 150 mL), dried over anhydrous Na_2SO_4, and filtered. The filtrate was evaporated and dried under vacuum at room temperature. The residue was re-dissolved in THF, precipitated from hexanes, and dried under vacuum at room temperature for 24 h. Conversion (%) (NMR) = 100%. Polymer yield = 89%.

^{1}H NMR (300 MHz, DMSO-d_6) [**Figure 2.1(B)**]: δ (ppm) = 1.45 (m, 3H$_d$), 1.70-1.72 (d, 3H$_g$), 4.75 (q, 1H$_h$), 5.1-5.2 (m, 2H$_b$ + 1H$_c$), 7.35 (m, 5H$_a$)

M_n(NMR) = 3,700 g mol^{-1}, M_n(GPC) = 5,700 g mol^{-1}, M_w / M_n = 1.41.

2.2.5. Typical Synthesis of PDLLA$_{42}$-C(O)CH(CH$_3$)SC(S)OC$_2$H$_5$ (PDLLA$_{42}$-X) (run 5, Table 2.1)

In a dried and nitrogen purged round-bottom flask, 2.95 g [7.97 × 10^{-4} mol calculated on the basis of molecular weight (3,700 g mol^{-1}) obtained from ^{1}H NMR] of PDLLA-Br and 0.5 g of potassium *O*-ethyl xanthate (3.12 × 10^{-3} mol) were dried and degassed by three freeze-pump-thaw cycles. In another dried and nitrogen purged round-bottom flask, 4.5 mL (4.4 g, 5.56 × 10^{-2} mol) pyridine was dissolved in 30 mL CH_2Cl_2 while stirring under nitrogen. This solution was added to the previous reaction mixture during stirring under nitrogen. The reaction mixture was stirred at room temperature for 36 h and diluted with 100 mL CH_2Cl_2. The solution was washed consecutively with saturated NH_4Cl solution (4 × 50 mL), saturated $NaHCO_3$ solution (4 × 50 mL), and water (4 × 100 mL). The organic layer was dried over anhydrous $MgSO_4$, filtered and the filtrate was evaporated to dryness. The residue was re-dissolved in THF, precipitated from hexane and dried under vacuum at room temperature for 24 h. Conversion (%) (NMR) = 100%. Polymer yield = 80%.

^{1}H NMR (300 MHz, DMSO-d_6) [**Figure 2.1(C)**]: δ (ppm) = 1.45 (m, 3H$_d$+3H$_g$+3H$_j$), 4.44 (q, 1H$_h$), 4.59 (q, 2H$_i$), 5.2 (m, 2H$_b$ + 1H$_c$), 7.35 (m, 5H$_a$)

M_n(NMR) = 3,900 g mol^{-1}, M_n(GPC) = 6,000 g mol^{-1}, M_w/ M_n = 1.43.

2.2.6 Synthesis of the Block Copolymer PDLLA$_{42}$-*b*-PNVP$_{37}$ (run 1, Table 2.2)

In a dried and nitrogen purged Schlenk tube, 0.5 g [1.29×10^{-4} mol, calculated on the basis of molecular weight (3,900 g mol^{-1}) obtained from ^{1}H NMR] of PDLLA-X was dissolved in 4 mL THF. To it, 0.95 mL (0.99 g, 8.89×10^{-3}mol) of NVP, and 7.2 mg (4.41×10^{-5} mol) of AIBN were added. A homogeneous solution was obtained after stirring and degassed under nitrogen for 45 min. The Schlenk tube was then immersed in an oil bath preheated at 80 ºC for 24 h. The reaction was stopped by freezing the reaction mixture with liquid nitrogen. A small portion of the polymerization mixture was used to determine the monomer conversion by ^{1}H NMR. The rest of the polymerization mixture was dissolved in 20 mL THF, precipitated from 350 mL hexane and dried under vacuum at room temperature for 24 h. The resultant polymer was soluble in water. Observed monomer conversion by ^{1}H NMR = 84%.

^{1}H NMR (300 MHz, $CDCl_3$): δ (ppm) = 1.2-1.8 (m, $3H_d+2H_k+3H_g+3H_j$), 1.8-2.2 (m, $2H_q$), 2.2-2.5 (m, $2H_r$), 3.0-3.5 (m, $2H_p$), 3.5-4.0 (m, $1H_l$), 5.2 (m, $2H_b+1H_c$), 7.2-7.4 (m, $5H_a$).

M_n(GPC) = 10,200 g mol^{-1}, M_w / M_n = 1. 36.

2.2.7. Synthesis of the Block Copolymer PDLLA$_{42}$-*b*-PNVP$_{63}$ (run 2, Table 2.2)

This block copolymer was prepared as mentioned in the previous paragraph using 0.4 g [1.03×10^{-4} mol, calculated on the basis of molecular weight (3,900 g mol^{-1}) obtained from ^{1}H NMR] of PDLLA-X, 1.52 mL (1.58 g, 1.42×10^{-4} mol) of NVP, 5.8 mg (3.5×10^{-5} mol) of AIBN, and 4 mL THF. Observed monomer conversion by ^{1}H NMR = 76%.

^{1}H NMR (300 MHz, $CDCl_3$ [**Figure 2.3(A)]:** δ (ppm) = 1.2-1.8 (m, $3H_d$+$2H_k$+$3H_g$ +$3H_j$), 1.8-2.2 (m, $2H_q$), 2.2-2.5 (m, $2H_r$), 3.0-3.5 (m, $2H_p$), 3.5-4.0 (m, $1H_l$), 5.2 (m, $2H_b$+$1H_c$), 7.2-7.4 (m, $5H_a$).

M_n(GPC) = 13,100 g mol^{-1}, M_w / M_n = 1.41.

2.2.8 Degradation of PDLLA Block in the Block Copolymers Obtained in the Kinetic Study

In a typical degradation study, 50 mg block copolymer and 10 mL 0.5 M NaOH solution prepared in 40% (v/v) methanol-water mixture were taken in a Schlenk tube fitted with a condenser and heated in a oil-bath at 65^{o}C for 6 days. Resultant reaction mixture was neutralized with 5% HCl solution. The neutralized reaction mixture was evaporated to dryness followed by the extraction with dichloromethane. The dichloromethane soluble part was evaporated to dryness followed by the drying under vacuum at room temperature for 24 h. The dried polymer was characterized by ^{1}H NMR in $CDCl_3$ and GPC.

2.2.9 Drug Loading and Release Studies

20 mg of $PDLLA_{42}$-*b*-$PNVP_{63}$ block copolymer was dissolved in 10.0 mL deionized water and stirred 3 h at room temperature (RT). 5.0 mg of Methotrexate (MTX) drug was dissolved in 0.3 mL DMF. After well mixing, the drug solution was then added drop wise into polymeric solution under stirring and stirring continued overnight at RT. The drug loaded polymeric solution was put into a dialysis tube (MW cut off = 3500 Da) and dialyzed against 500 mL distilled water, and distilled water was replaced initially every 3 h for 12h followed by every 6 h for 48 h. The dialyzed drug-loaded micelle solution was lyophilized, dissolved in DMF (1 mg / mL) and analyzed by UV

absorbance at 308 nm, using a standard calibration curve [**Figure 2.17**] experimentally obtained with solutions containing different concentrations of MTX in DMF. Drug loading content (DLC) and drug loading efficiency (DLE) were calculated according to the following formula:

Drug loading content (DLC) (wt. %) = (weight of loaded drug / weight of polymer) ×100%

Drug loading efficiency (DLE) (wt. %) = (weight of loaded drug / weight of the drug in the feed) ×100%

For drug release study, 5 mg of MTX loaded polymer sample was dissolved in 2.0 mL PBS (pH = 7.4/6.4) solution and transferred into dialysis tubing (MW cut-off: 3500 Da). The tubing was placed into 50 mL PBS solution. The system was shaken at 60 rpm at 37°C. At predetermined interval, 2.0 mL PBS solution was taken out and volume of solution was kept constant by adding 2.0 mL PBS solution after each sampling. The amount of MTX released from micelles at different time intervals was measured by UV absorbance at 308 nm.

2.2.10 Cell Lines and Cell Culture

Dalton lymphoma (DL) celles were transplanted in the peritoneum of AKR (H2k) mice by periodic transfer of tumor cells via intraperitoneal injections. [Hira *et al*. (2014)] Human Burkitt's lymphoma cell line Raji was purchased from American Type Culture Collection (ATCC), Manassas, USA. The cells were cultured in RPMI 1640 (Invitrogen, Carlsbad, CA, USA) supplemented with 10% fetal bovine serum (Hyclone, Logan, UT, USA), 100 U/mL penicillin, and 100 µg/mL streptomycin (Invitrogen, Carlsbad, CA, USA), henceforth, called as complete medium. The cell lines used in the study were free from mycoplasma.

2.2.11 Development of MTX-resistant DL and Raji cells

DL and Raji cells were grown in complete medium in the presence of 500 nM MTX at 37 °C and 5% CO_2. MTX resistance cells were assessed by observing the size of the cells and nuclei, and dihydrofolate reductase activity. [Ohnoshi *et al*. (1985)] Activity of dihydrofolate in the tumor cell was determined by preparing cell extracts as described earlier. [Cowan *et al*. (1984)] Cells were harvested, washed three times with Hanks' Balanced Salt Solution (HBSS), and suspended in ice-cold 50 mM potassium phosphate (pH 7.0). This suspension was disrupted with a probe sonicator for 5 min. The cell lysate was centrifuged at 100000*g* for 60 min at 4°C in order to yield supernatant called the cell extract. Folate reductase activity in the cell extract was determined using dihydrofolate reductase assay kit.

2.2.12 *In Vitro* Cell Viability Assay

Effect of free MTX or, MTX-loaded $PDLLA_{42}$-*b*-$PNVP_{63}$ amphiphilic block copolymer micelles on the viability of tumor cells, human lymphocytes or, dendritic cells (DC) was evaluated by a colorimetric XTT (sodium 3-[1-(phenylaminocarbonyl)-3,4-tetrazolium]-bis(4-methoxy-6-nitro) benzene sulfonic acid hydrate) assay (Roche Molecular Biochemicals, Indianapolis, USA). Lymphocytes were collected from peripheral blood by centrifugation in Ficoll-Hypaque. Dendritic cells were generated by culturing monocytes with recombinant human GM-CSF and IL-4 for 7 days as described elsewhere. [Hira *et al*. (2014)] Tumor cells, lymphocytes or, DC were plated (5×10^3 cells/well) in a 96-well plate and exposed to serial concentrations of (25, 50, 100 and 200 μM) free MTX or, MTX-loaded $PDLLA_{42}$-*b*-$PNVP_{63}$ amphiphilic block copolymer micelles and incubated at 37 °C, 5% CO_2, for 18 h. Optical density (OD)

was measured at 450 nm using Synergy HT Multi-Mode Micro plate Reader BioTek, USA. [Thomas *et al*. (2005)] The data was presented as the percentage of viable cell calculated from the following formula:

$$\% \text{ Cell Viability} = \frac{\text{Experimental } OD_{450}}{\text{Control } OD_{450}} \times 100$$

2.2.13 *In Vitro* Cytotoxicity Assay

The lytic activity of MTX-loaded $PDLLA_{42}$-*b*-$PNVP_{63}$ amphiphilic block copolymer micelles against tumor cells was measured by non-radioactive cytotoxicity assay using the CytoTox 96 Non-Radioactive Cytotoxicity assay kit from Promega, USA. [Manna *et al*. (2013)] Target cells (5×10^3) were added to 96-well tissue culture plate and exposed to serial concentrations of (50, 100, 150, 200 and 250 μM) free MTX, polymeric micelle or, MTX-loaded $PDLLA_{42}$-*b*-$PNVP_{63}$ micelles solution and incubated for 18h at 37ºC, 5% CO_2. Percent-specific lysis was determined using the following formula:

$$\% \text{ Cytotoxicity} = \frac{(\text{Experimental - Effector Spontaneous - Target Spontaneous})}{(\text{Target Maximum - Target Spontaneous})} \times 100$$

.

2.2.14 Tumor Cell Proliferation Assay

Growth inhibitory potential of free MTX, MTX-loaded $PDLLA_{42}$-*b*-$PNVP_{63}$ amphiphilic block copolymer micelles against parental and MTX-resistant DL and Raji cells was studied by MTT assay. In a 96-well tissue culture plate, 5×10^3 cells/well were added and exposed to serial concentrations of free MTX and MTX-loaded $PDLLA_{42}$-*b*-$PNVP_{63}$ micelles. Plates were incubated at 37 ºC, 5% CO_2 for 48 h. The cell proliferation was measured by CellTiter 96 Non-Radioactive Cell Proliferation Assay

(MTT) kit from Promega, USA. The data presented as the percentage of inhibition of tumor cells and was calculated from the following formula:

$$\% \text{ Growth Inhibition} = [1 - \frac{\text{Experimental } OD_{570}}{\text{Target } OD_{570}}] \times 100$$

where, experimental OD value is the reading of tumor cells exposed to various concentrations of MTX and the target OD value is the value of tumor cell only, cultured in absence of the drug. [Hira *et al*. (2014)]

2.2.15 Detection of Apoptosis

Apoptotic cell death in parental and MTX resistant (MTX-R) DL or, Raji cells by free MTX or, MTX-loaded $PDLLA_{42}$-*b*-$PNVP_{63}$ amphiphilic block copolymer micelles were assessed by binding FITC-conjugated Annexin V. After 18 h of incubation, apoptotic cells were analyzed by staining with FITC-conjugated Annexin V and propidium iodide (PI) for 20 minutes in ice-cold PBS. Cells were washed in Annexin buffer and were mounted on microscope slides with a drop of mounting medium to reduce fluorescence photo bleaching. The FITC-conjugated Annexin V positive cells were visualized under a fluorescence microscope (Nikon Eclipse 80i, Nikon, Japan).

2.2.16 Hemolysis Assay

For time dependent kinetics, a concentration of 100 μM MTX or, MTX-loaded $PDLLA_{42}$-*b*-$PNVP_{63}$ micelles was incubated with the blood sample. For concentration dependent kinetics, the blood sample was incubated with varying concentrations of the MTX or, MTX-loaded $PDLLA_{42}$-*b*-$PNVP_{63}$ micelles for 4 h. Hemolysis assay was performed according to the standard protocol. [Kuznetsova *et al*. (2012)] In brief, an aliquot of each blood sample was centrifuged at 600 g for 5 min. 25 µL plasma aliquot

was diluted with 225 µL Drabkin's reagent (Sigma) in a 96-well plate and mixed for 2 min under lateral agitation (300 rpm). After 10 minutes equilibration at room temperature, optical density was recorded at 540 nm in Synergy HT Multi-Mode Micro plate Reader BioTek, USA. Blood hemoglobin was determined by measuring the absorbance of 100-fold dilution of the whole blood in Drabkin's reagent at 540 nm. Saponin (2 mg/mL final blood concentration) and PBS were used as positive and negative control, respectively. A sample of plasma without additives was considered as basal conditions. Standard calibration curve was obtained with the solutions containing 0.07 to 3.8 mg/mL bovine hemoglobin (Sigma) treated with Drabkin's reagent. The results are presented as percent hemolysis indicating the free plasma hemoglobin (mg/mL) and was measured as released hemoglobin divided by the total blood hemoglobin (mg/mL) multiplied by 100. All measurements were performed in triplicate.

2.2.17 Statistical Analysis

The mean ± SD was calculated from the data collected for each experimental groups (n = 3-5). Differences between groups were analyzed by unpaired Student's t-test and one- or, two-way ANOVA analysis of variance depending on the requirement. This was followed by Holm-Sidak posthoc multiple comparison tests using PRISM statistical analysis software (Graph Pad Software, Inc., San Diego, CA, USA). Significant differences among groups were calculated at $p < 0.05$ or, less. The statistical significance of differences in survival of the mice in different groups was determined by the log-rank test using Graph Pad PRISM software.

2.3 Results and Discussion

2.3.1 Synthesis of PDLLA-b-PNVP Diblock Copolymers

A new method for the synthesis of PDLLA-*b*-PNVP *via* the combination of ROP and xanthate-mediated RAFT polymerization is shown in [**Scheme 2.1**]. PDLLA-OH has first been synthesized via ROP of DLLA in bulk at 150 ^{o}C using benzyl alcohol as initiator and $Sn(Oct)_2$ as the catalyst. The results of the synthesis and characterization of PDLLA-OH prepared using two different DLLA / benzyl alcohol feed ratios are included in [**Table 2.1**(**Runs 1 and 2**)]. Polymer yields are almost quantitative. The observed molecular weights are increased with the increase in the feed ratio of DLLA / benzyl alcohol, as expected. GPC chromatogram [**Figure 2.2(a)**] of **run 1**(**Table 2.1**) is unimodal with M_n (GPC) = 4,400 g mol^{-1} and PDI = 1.55. But, the GPC chromatogram of **run 2** [**Table 2.1**] is unimodal with a small hump at the higher molecular weight end. The observed difference in molecular weights determined by ^{1}H NMR [M_n(NMR)] and GPC [M_n(GPC)] is due to calibration of M_n(GPC) against PMMA standards. The typical ^{1}H NMR spectra of the PDLLA-OH polymer obtained in **run 1** [**Table 2.1**] is shown in **Figure 2.1(A)**.

Then, PDLLA-OH polymers are reacted with 2-bromopropionyl bromide in the presence of triethylamine to prepare 2-bromopropionyl-terminated poly(D,L-lactide) (PDLLA-Br) [**Scheme 2.1**]. The results of the synthesis and characterization of PDLLA-Br polymers from the corresponding PDLLA-OH polymers are included in **runs 3** and **4** [**Table 2.1**]. The typical ^{1}H NMR spectra of the resultant PDLLA-Br polymer obtained in **run 3** is shown in **Figure 2.1(B)**. The incorporation of the 2-bromopropionyl group is evidenced from the appearance of methine (*h*) and methyl (*g*) protons of 2-bromopropionyl end-group of the PDLLA-Br at around 4.72 and 1.72

ppm, respectively. The calculated conversion (%) of –OH end-group into its corresponding 2-bromopropionyl end-group obtained by comparing the peak area of methyl (*g*) protons of 2-bromopropionyl end-group with that of the aromatic proton (*a*) of the polymer chain-end at ~ 7.4 ppm is ~ 100%. The M_n(NMR) of this polymer calculated by dividing average peak area of methylene protons (*c*) of the PDLLA backbone chain by the peak area of (*a*) is 3704 g mol^{-1}. The corresponding observed M_n(GPC) and PDI are 5,700 g mol^{-1} and 1.41, respectively [**Figure 2.2(a)**].

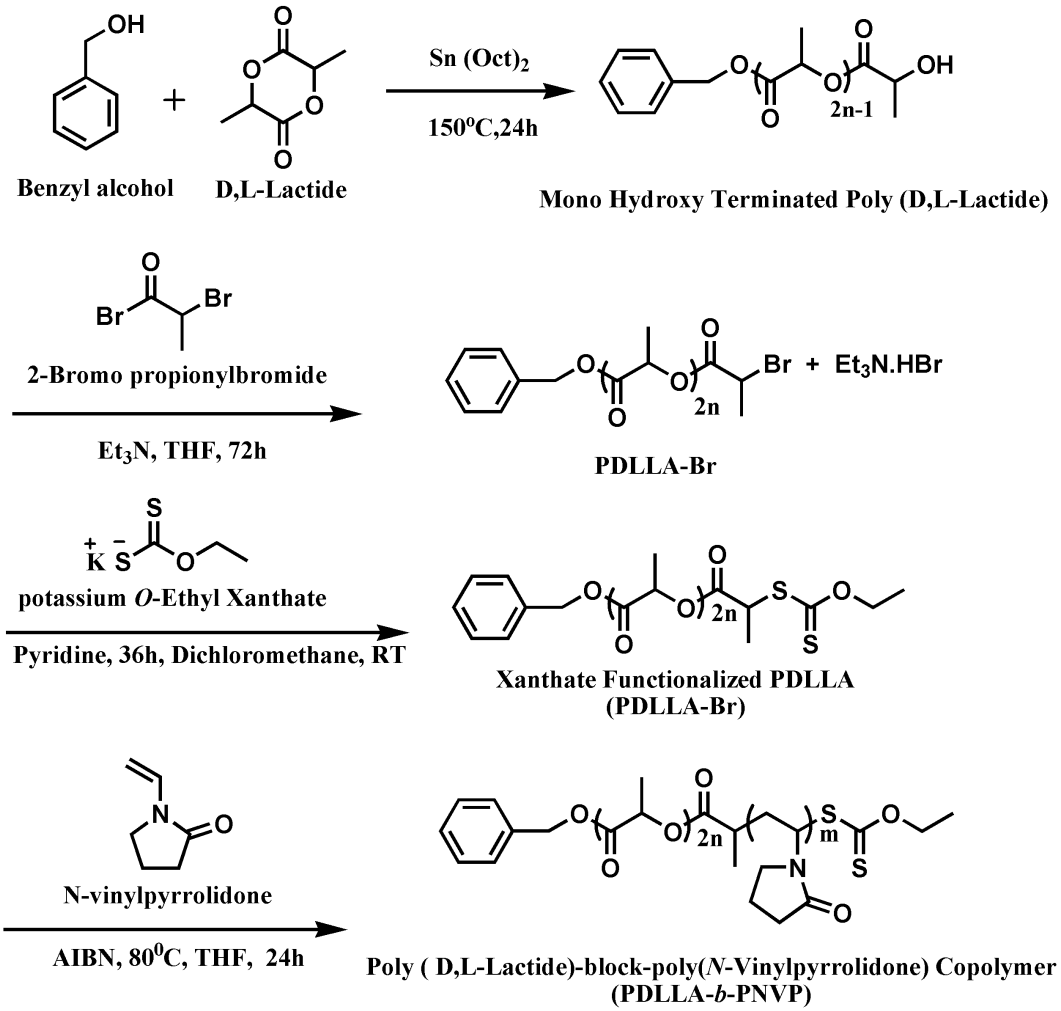

Scheme 2.1. Synthesis of PDLLA-*b*-PNVP block copolymers via ROP and xanthate mediated RAFT polymerization methods.

Similarly, quantitative conversion of –OH functional group into its corresponding 2-bromopropionyl group is also observed for the higher molecular weight PDLLA-OH [**run 4**, **Table 2.1**]. PDLLA-Br polymers are then reacted with potassium-*O*-ethyl xanthate to convert the bromo end-group into the corresponding xanthates (PDLLA-X) by ionic substitution reaction [**Scheme 2.1**]. The results of the synthesis and characterization of PDLLA-X polymers from the corresponding PDLLA-Br polymers are included in **runs 5** and **6** [**Table 2.1**]. The typical ^{1}H NMR spectrum of the resultant PDLLA-X polymer obtained in **run 5** is shown in **Figure 2.1(C)**. The conversion of bromo end-group into the corresponding xanthate end-group is confirmed by the appearance of the new characteristic peak attributed to the methylene proton (*i)* of the xanthate end group at 4.6 ppm. The corresponding peaks of the methyl protons of the xanthate end-group (*j*) and of the propionyl group (*g*) are overlapped within the peak of the methyl protons (*d*) of the PDLLA backbone chain. We also did not able to find a separate peak of methyl protons (*d*) in $CDCl_3$ solvent.

Table 2.1 Synthesis of PDLLA-X Macro-chain Transfer Agents

Run	Sample	% Yield[a]	Conv(%)[b] (nmr.)	M_n[b](NMR) ($gmol^{-1}$)	M_n[c](GPC) ($gmol^{-1}$)	PDI[c] (GPC)	Comments
1	$PDLLA_{42}$-OH [d]	79	98.7	3600	4400	1.55	Unimodal
2	$PDLLA_{64}$-OH [d]	78	97.7	6600	9900	1.67	Unimodal with small hump at high mol.wt. end
3	$PDLLA_{42}$-Br [e]	89	100	3700	5700	1.41	Unimodal
4	$PDLLA_{64}$-Br [e]	94	100	7000	9200	2.30	Unimodalwith small hump at high mol.wt. end
5	$PDLLA_{42}$-X [f]	80	100	3990	6000	1.43	Unimodal
6	$PDLLA_{64}$-X [f]	78	100	6800	8800	1.46	Unimodalwith small hump at high mol.wt. end

[a] Determined by gravimetry [b] Determined by ^{1}H NMR; [c] Determined by GPC (DMF, 0.5 mL/min, 40 ^{o}C) calibrated against PMMA standards.[d] Bulk polymerization using 5 g (34.7 mmol) D,L-lactide, 25 mg (6.47×10^{-2} mmol) $Sn(OCt)_{2)}$ in the presence of benzyl alcohol at 150 ^{o}C for 16 h; [e] Using PDLLA-OH :triethylamine: 2-bromopropionylbromide: 1:2.5:2 in THF at RT for 72 h; [f] Using PDLLA-Br : potassium-*O*-ethyl xanthate : pyridine :: 1 : 3 : 53 in dichloromethane at RT for 36. h;

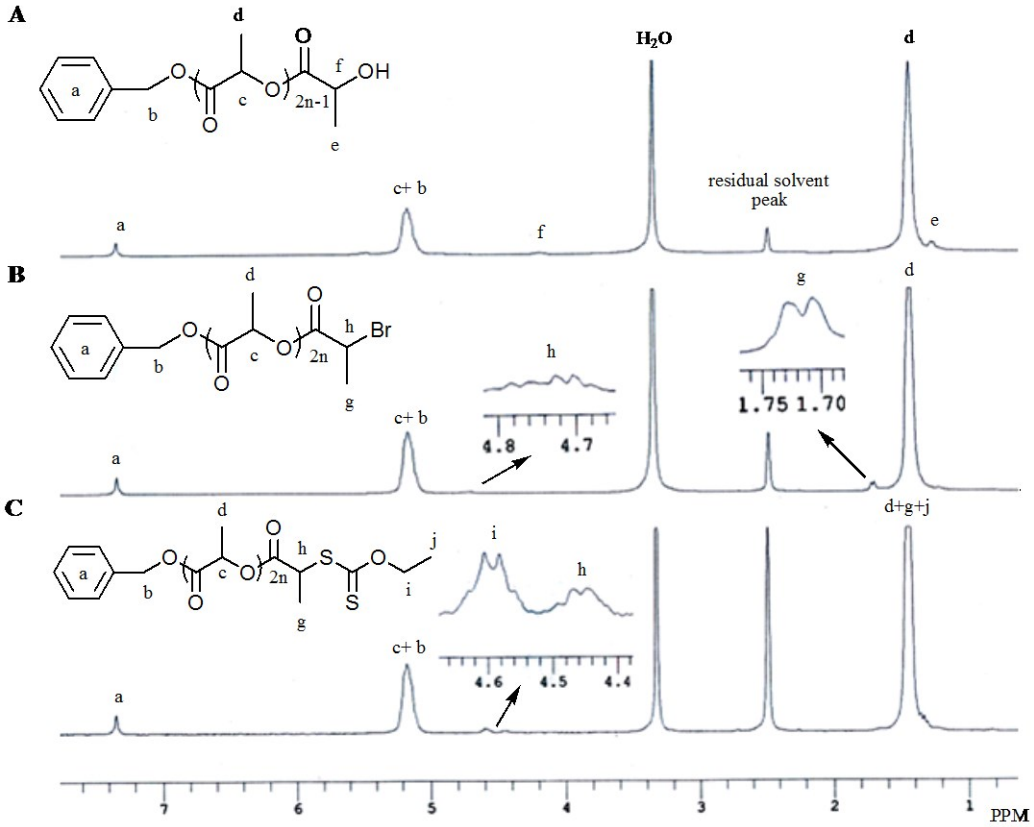

Figure 2.1 ^{1}H NMR spectra of (**A**) PDLLA$_{42}$-OH (**run 1**), (**B**) PDLLA$_{42}$-Br (**run 3**) and (**C**) PDLLA$_{42}$-X (**run 5**) in DMSO-d_6 at room temperature (**Table 2.1**).

The calculated conversion (%) of –Br end-group into its corresponding xanthate end-group obtained by comparing peak area of methine protons (*h*) of the propionyl group with the methylene protons (*i*) of the xanthate end-group is ~ 100% [**Figure 2.1(C)**]. Inclusion of xanthate group (-S-(C=S)-) at the chain-end of PDLLA-X is also supported by the observation of the characteristic UV absorption peak at λ ~ 280 nm in its THF solution. The M_n(NMR) of this polymer calculated from its ^{1}H NMR by comparing the peak area of '*c*' by the peak area of '*a*' is observed at 3,900 g mol^{-1} [**Figure 2.1(C)**]. The corresponding observed M_n(GPC) and PDI are 6,000 g mol^{-1}, and 1.43, respectively [**Figure 2.2(a)**]. Therefore, the molecular weights and PDI values of the converted PDLLA-X polymers are almost close to the value observed for the

corresponding PDLLA-Br polymers. Similarly, quantitative conversion (%) of –Br end-group into the corresponding xanthate end-group is also observed with the higher molecular weight PDLLA-Br (**run 6**, **Table 2.1**).Therefore, the quantitative conversion of –Br end-group into its corresponding xanthate end-group is observed for both PDLLA studied here irrespective of their molecular weights.

Then, PDLLA-X is used as a macro-chain transfer agent for the xanthate mediated RAFT polymerization of NVP in THF using [PDLLA-X]: [AIBN] = 1: 0.25 at 80 ^{o}C for 24 h. The results of the synthesis and characterization of PDLLA-*b*-PNVP block copolymers from the corresponding PDLLA-X polymers are shown in **Table 2.2**.

Table 2.2 Characteristic Data of PDLLA-*b*-PNVP Block Copolymers[a]

Run	Block Copolymers	PDLLA$_x$-X (*M*n/PDI)	NVP[b] (equiv)	Conv.[c] (%)	$M_{n\,(theor)}$[d] (g mol^{-1})	$M_{n\,(NMR)}$[e] (g mol^{-1})	$M_{n\,(GPC)}$[f] (g mol^{-1})	PDI[f]	X_{PNVP}[g] (NMR)	X_{PNVP}[g] (GPC)	CMC(mg/mL) (Fluorescence)
1	PDLLA$_{42}$-*b*-PNVP$_{37}$	PDLLA$_{42}$-X (6000/1.43)	50	84	8548	7100	10200	1.36	0.46	0.40	0.0024
2	PDLLA$_{42}$-*b*-PNVP$_{63}$	PDLLA$_{42}$-X (6000/1.43)	100	78	12548	10700	13100	1.41	0.64	0.53	0.0034
3	PDLLA$_{42}$-*b*-PNVP$_{120}$	PDLLA$_{42}$-X (6000/1.43)	200	67	18772	16500	19400	1.52	0.76	0.69	0.0060
4	PDLLA$_{64}$-*b*-PNVP$_{24}$	PDLLA$_{64}$-X (8800/1.46)	100	73	14884	14700	11800	1.51	0.58	0.22	0.0021
5	PDLLA$_{64}$-*b*-PNVP$_{48}$	PDLLA$_{64}$-X (8800/1.46)	200	78	24109	22700	14500	1.60	0.73	0.37	0.0034

[a] Using 0.25 equivalent AIBN with respect to PDLLA-X macroinitiator in THF at 80 ^{o}C for 24h; [b] With respect to PDLLA-X macroinitiator; [c] Conversion was determined by comparing the peak area of the residual vinylic sigments of the NVP monomer at ~4.3 - 4.4 ppm (2H) and ~7.0 - 7.1ppm (1H) with the peak area of methylene proton of the PNVP block of the polymer at ~3 .0-3.4 ppm (2H) by use of ^{1}H NMR; [d] M_n(theor) = ^{1}H NMR mol. wt. of PDLLA-X + ([NVP]$_o$/ [PDLL A-X] × fraction conversion of NVP × mol. wt. of NVP); [e] determine from ^{1}H NMR by compairing the of PDLLA block at ~5.2ppm with the methylene proton of PNVP block at ~3.0 - 3.4 ppm; [f] Determined by GPC(DMF, 0.5 mL/min, 40 ^{o}C) calibrated against PMMA standards; [g] X_{PNVP} = mol-fraction of PNVP.

Runs 1, **2** and **3**, correspond to 50, 100, and 200 equivalents of NVP monomer loading with respect to PDLLA$_{42}$-X macro-chain transfer agent, respectively. Molecular weights of the resulted block copolymers are increased with the increase in the monomer loading as expected [**Table 2.2** and **Figure 2.2(b)**]. The observed mole fraction of PNVP block in

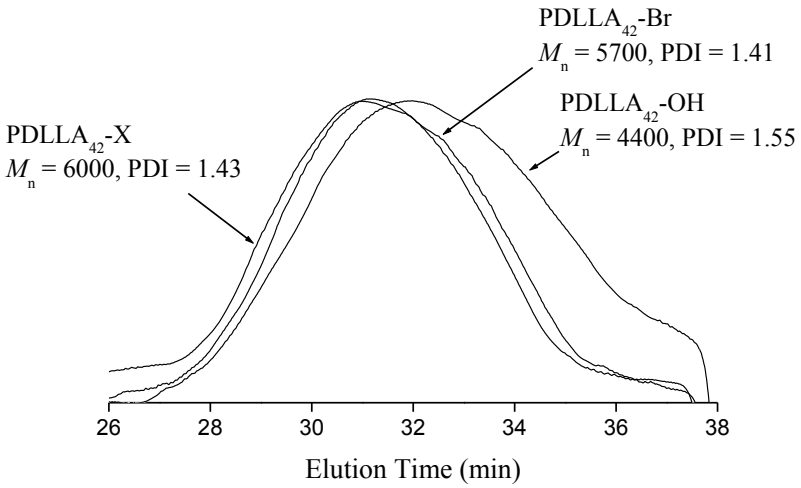

(a)

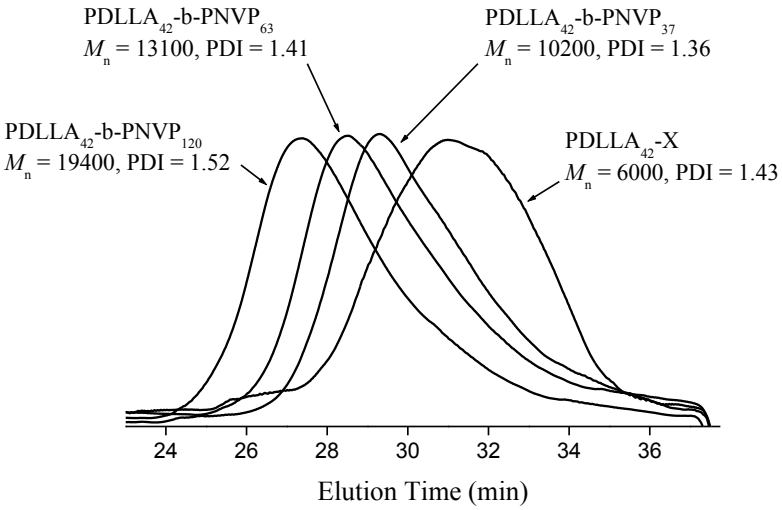

(b)

Figure 2.2(a) Gel permeation chromatograms of PDLLA$_{42}$-OH (**run 1**), PDLLA$_{42}$-Br (**run 3**) and PDLLA$_{42}$-X (**run 5)** [**Table 2.1**]. **(b)** Gel permeation chromatograms of macro-chain transfer agent PDLLA$_{42}$-X and the resulted block copolymers PDLLA$_{42}$-*b*-PNVP$_{37}$ (**run 1**), PDLLA$_{42}$-*b*-PNVP$_{63}$ (**run 2**), and PDLLA$_{42}$-*b*-PNVP$_{120}$ (**run 3**) [**Table 2.2**].

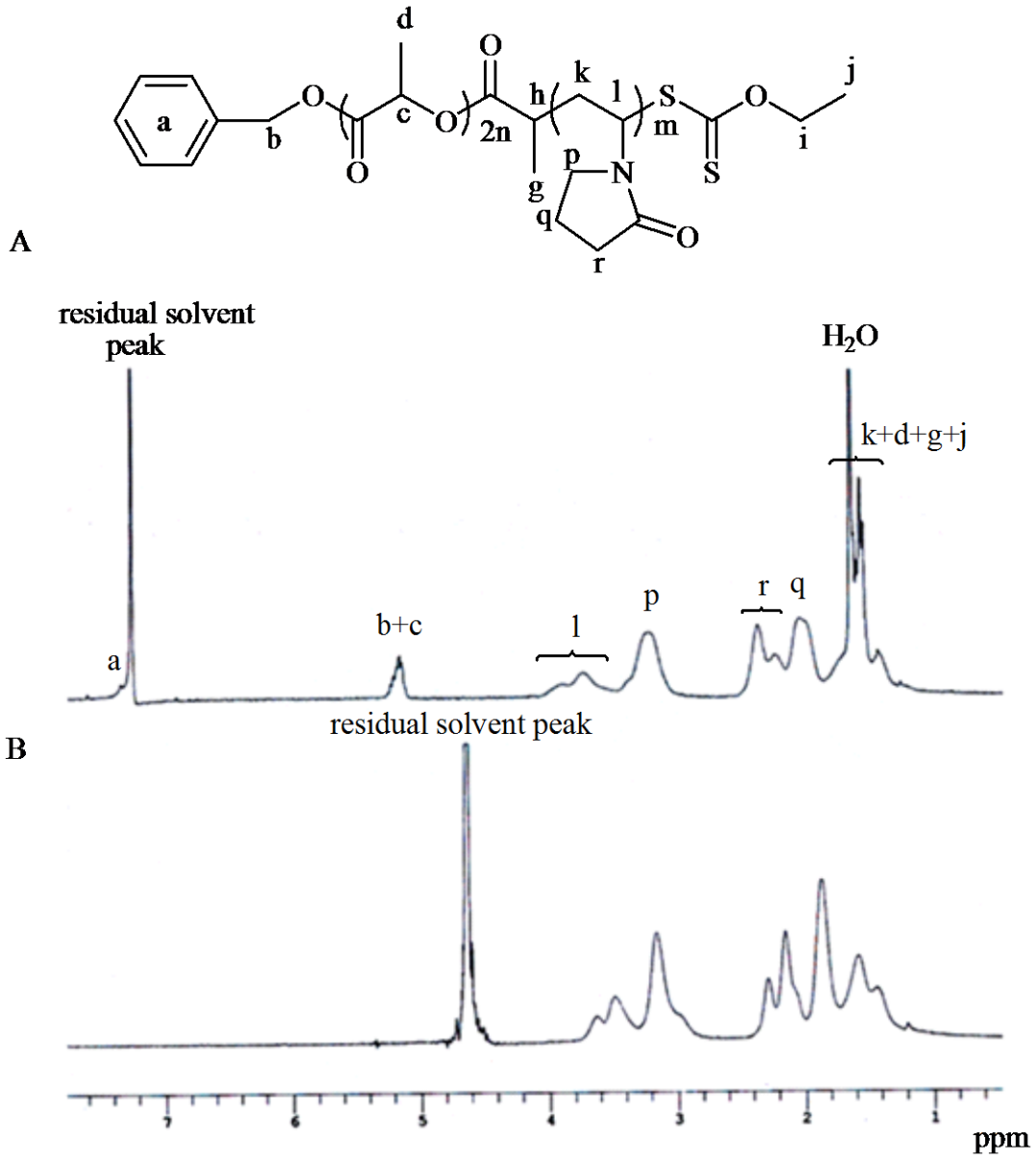

Figure 2.3 ^{1}H NMR spectra of PDLLA$_{42}$-*b*-PNVP$_{63}$ diblock copolymer in (**A**) *d*-chloroform, and (**B**) D_2O at room temperature.

these block copolymers calculated on the basis of ^{1}H NMR and GPC molecular weights are close to each other and within the range 0.40-0.76. Observed higher values of PNVP from ^{1}H NMR indicates the possible presence of PNVP homopolymer as impurities. The typical ^{1}H NMR spectrum of the block copolymer, prepared in **run 2**

[**Table 2.2**], in $CDCl_3$ [**Figure2.3(A)**], shows the characteristic peaks of the PDLLA block, Moreover, this spectrum shows the presence of the characteristic peaks of the PNVP backbone methine proton '*l*' at ~ 3.5-4.0 ppm, the methylene protons '*p*', '*r*', and '*q*' of the pyrrolidone ring at ~ 3.0-3.5, 2.2-2.5, and 1.8-2.2 ppm, respectively, apart from methylene protons '*k*' of the PNVP block overlapped between of ~ 1.2-1.8 ppm with methyl protons '*d*' of PDLLA block.

In **runs 4** and **5** [**Table 2.2**], high molecular weight $PDLLA_{64}$-X macro-chain transfer agent is used with 100 and 200 equivalent NVP monomer. Resulting two block copolymers have lower solubility in water than the above-mentioned three block copolymers. The observed mole fraction of PNVP block in these two block copolymers are 0.58 and 0.73 (calculated on the basis of ^{1}H NMR), respectively, and 0.22 and 0.37 (calculated on the basis of GPC molecular weights), respectively. The observed differences in mole fraction of PNVP block using these two methods may due to the formation of more PNVP homopolymers while using high molecular weight PDLLA-X macro RAFT agent and it is observable better using ^{1}H NMR than GPC method. Thus, the most successful occurrence of the chain extensions occurs with $PDLLA_{42}$-X having M_n(GPC) = 6,000 g mol^{-1} and PDI = 1.43.

Livingness of this polymerization system is checked by performing the kinetic study of the polymerization of NVP in THF at 80 ^oC using $PDLLA_{42}$-X macro chain-transfer agent with molar ratio [NVP]: [$PDLLA_{42}$-X]: [AIBN] = 100:1:0.25. The plot of the monomer conversion (%) and ln([M_o]/[M]) vs. time is shown in [**Figure 2.4(a)**]. Monomer conversion (%) is increased almost linearly up to 47.6% conversion. The corresponding plot of ln([M_o]/[M]) vs. time is also linear up to around 47.6% conversion.

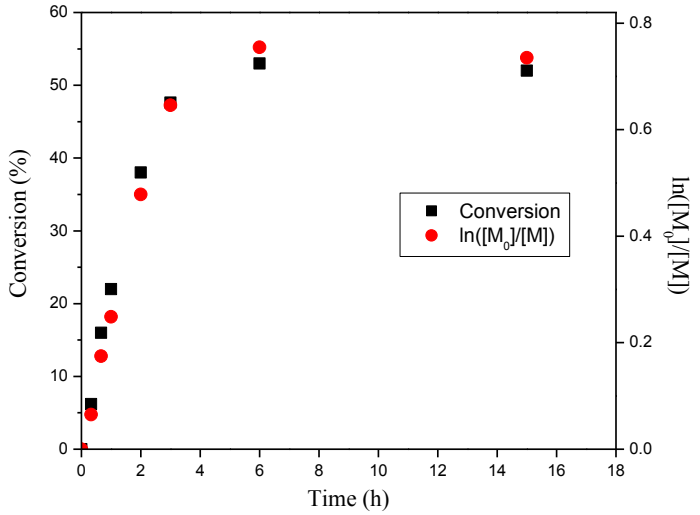

(a)

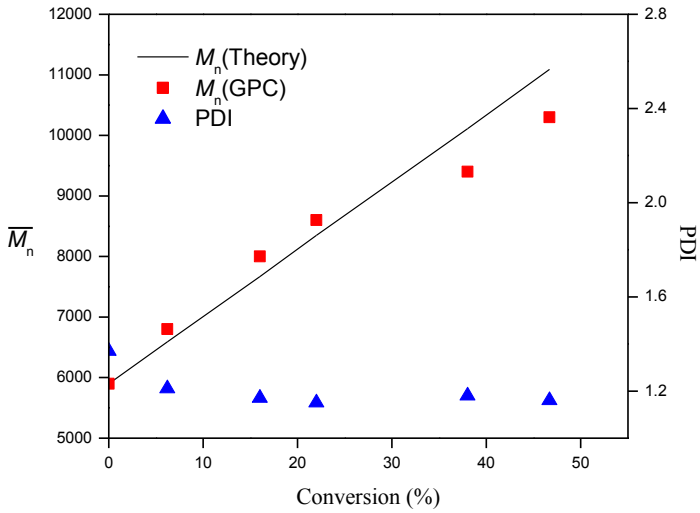

(b)

Figure 2.4(a) Plots of time vs. monomer conversion and ln([M_o]/[M]) (where [M_o]= concentration of the monomer at time t = 0 min and [M] = concentration of the monomer at the corresponding time) and **(b)** Plots of number-average molecular weight (M_n) and polydispersity (PDI) vs. monomer conversion in the polymerization of *N*-vinylpyrrolidone in THF using [NVP] : [PDLLA$_{42}$-X chain transfer agent] : [AIBN] = 100 : 1 : 0.25 at 80 ^oC

So, the pseudo-first order monomer conversion kinetics is followed up to around 47.6% conversions. The plot of M_n and PDI vs. monomer conversion (%) is shown in [**Figure 2.4(b)**]. M_n(GPC)] values of the resulting polymers increased linearly with monomer conversion (%).The corresponding overlay of the GPC chromatograms shows clearly the shifting of the molecular weight to the higher molecular weight with increase in conversion [**Figure 2.5**]. M_n(GPC) and the corresponding M_n(theor) are close to each other.

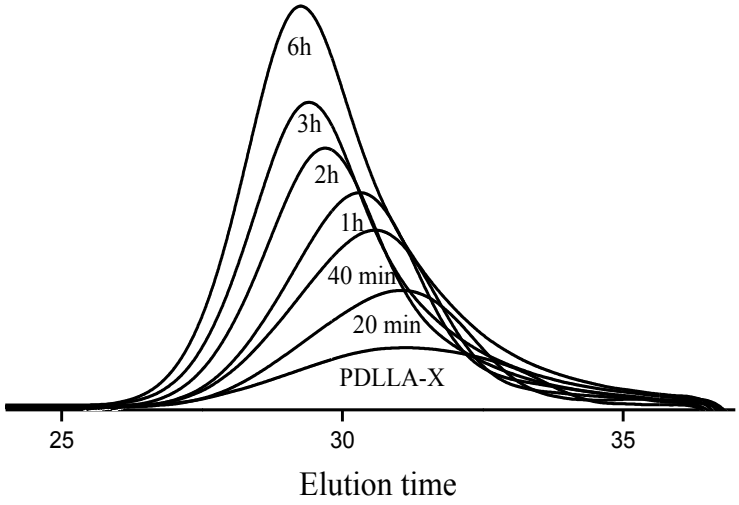

Figure 2.5 Overlay of the GPC chromatograms of the resultant polymers obtained in the kinetic study.

The corresponding PDI is decreased slightly with the increase in conversion up to 47.6%. These results for the polymerization of NVP using xanthate based RAFT macro chain-transfer agents are in good accordance with previously reported results in the literature. [Mishra *et al*. (2011), Wan *et al*. (2004)]

2.3.2 Degradation of PDLLA Block in the Block Copolymers

We have degraded the PDLLA block of the four block copolymers obtained from the above-mentioned kinetic study at 6.2% (20 min), 16% (40 min), 22% (60 min), and

46.7% (180 min) monomer conversions using 0.5 M NaOH solutions, prepared in 40% (v/v) methanol-water mixture, at 65 ^{o}C for 6 days. Resultant polymers are characterized by ^{1}H NMR and GPC. The absence of the characteristics peaks of PDLLA block and the presence of only characteristics peak of PNVP in the ^{1}H NMR of degraded block copolymer clearly indicate the complete degradation of PDLLA under the experimental conditions.[**Figure 2.6**] and PNVP homopolymer is formed out of the block copolymer hydrolysis.

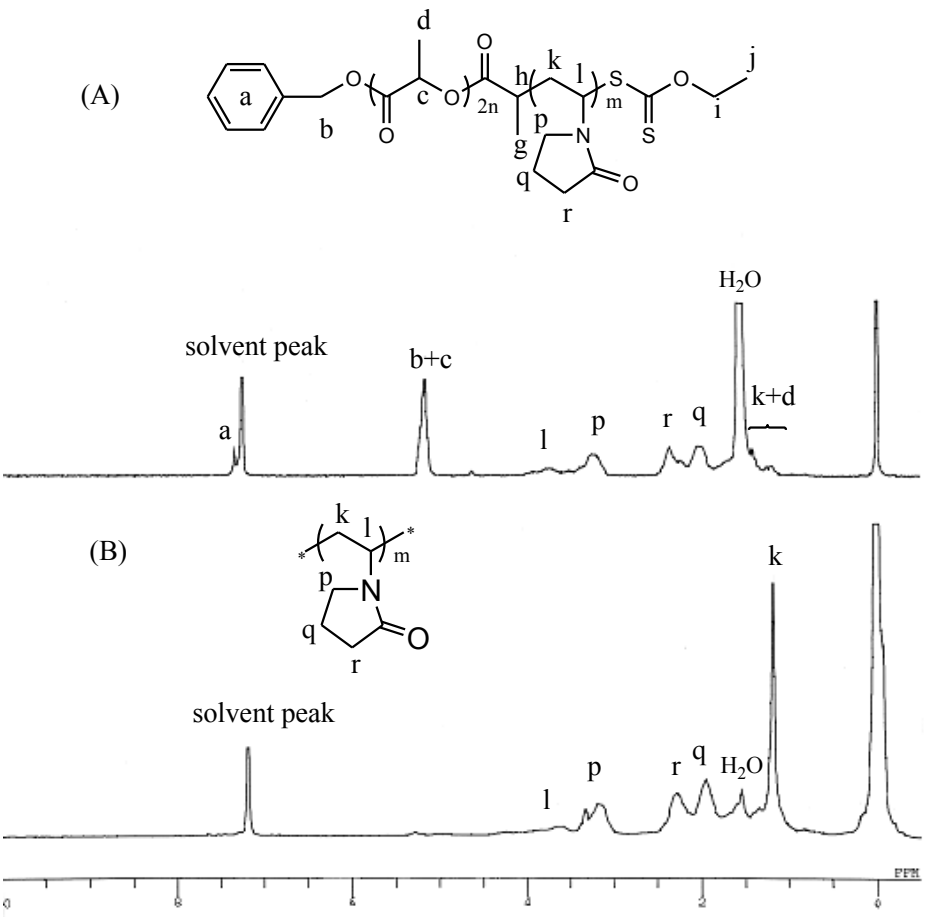

Figure 2.6 ^{1}H NMR spectra of polymers formed at t = 20 min in *d*-chloroform at room temperature: (**A**) before, and (**B**) after degradation.

Moreover, the observations of unimodal GPC chromatograms of theses PNVP polymers in all cases and the shifting of GPC chromatograms **[Figure 2.7**] towards higher molecular weight with the increase in conversion indicate clearly that length of PNVP block increases in the block copolymer with the gradual increase in the monomer conversion. Indeed, M_n(GPC) of PNVP block increases almost linearly with increase in conversion [**Figure 2.8**].

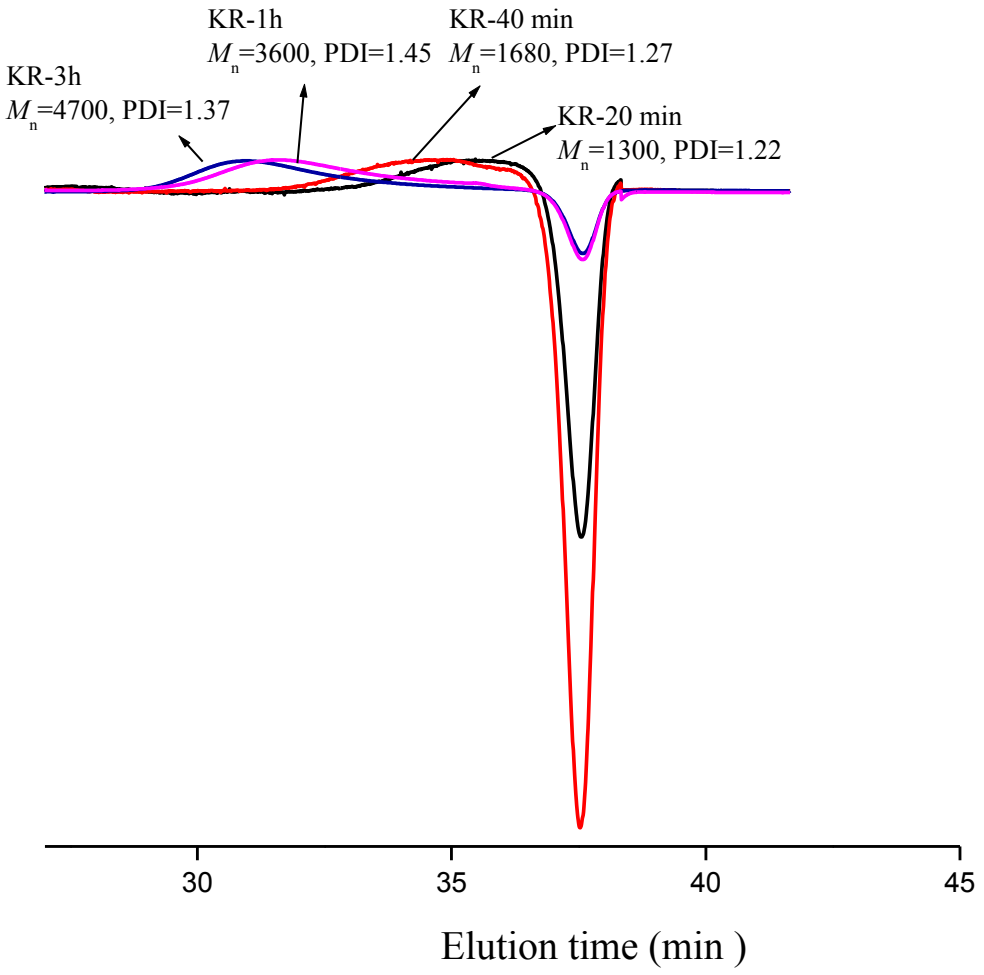

Figure 2.7 GPC Chromatograms of the corresponding PNVP polymers obtained from the degradation of the polymers formed in the kinetic study.

The corresponding PDI of the PNVP increases gradually with increase in the monomer conversion. It may be either due to the loss of xanthate moieties from the chain-end or, due to the considerable chain transfer reaction to monomer. All these results confirm the livingness of this polymerization system under the experimental conditions.

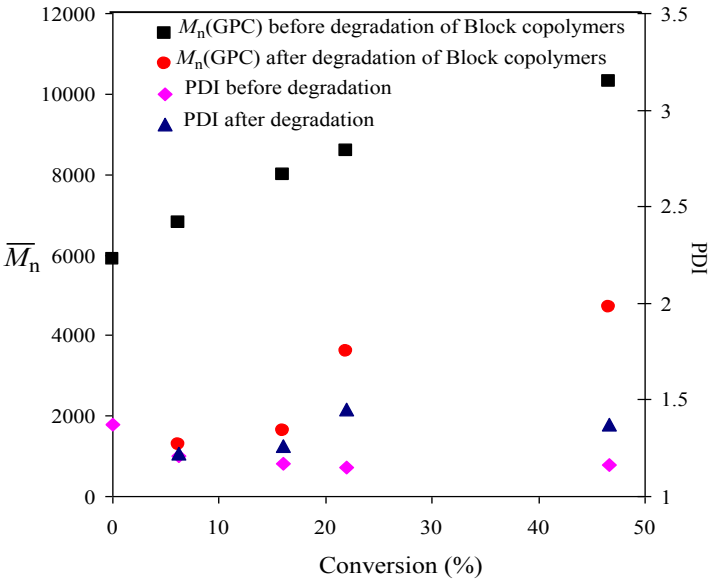

Figure 2.8 Plots of M_n(GPC) and PDI of the corresponding polymers obtained in the kinetic study before and after degradation *vs.* conversion.

2.3.3 Self-assembly of Amphiphilic PDLLA-b-PNVP Block Copolymers in Aqueous Solution

^{1}H NMR spectrum of PDLLA$_{42}$-*b*-PNVP$_{63}$ block copolymer in D_2O is shown in **Figure 2.3(B)**. Here, the peaks attributed to PDLLA, which are clearly observable in the corresponding spectrum taken in $CDCl_3$ [**Figure 2.3(A)**], are completely disappeared. This observation indicates the possible formation of micelles in water with PDLLA block as the cores and PNVP block as the shells. In order to determine the *cmc* of all

five block copolymers (**Table 2.2**) in water, fluorescence spectroscopy is used with pyrene as the probe. The typical fluorescence excitation spectra (300 - 360 nm) of

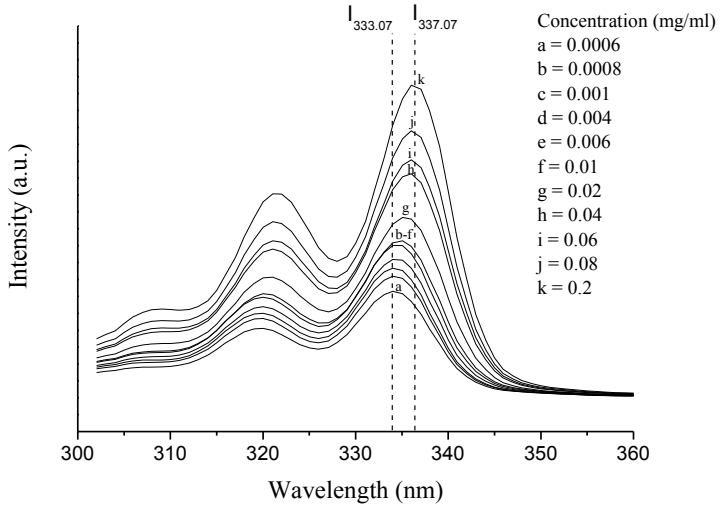

(a)

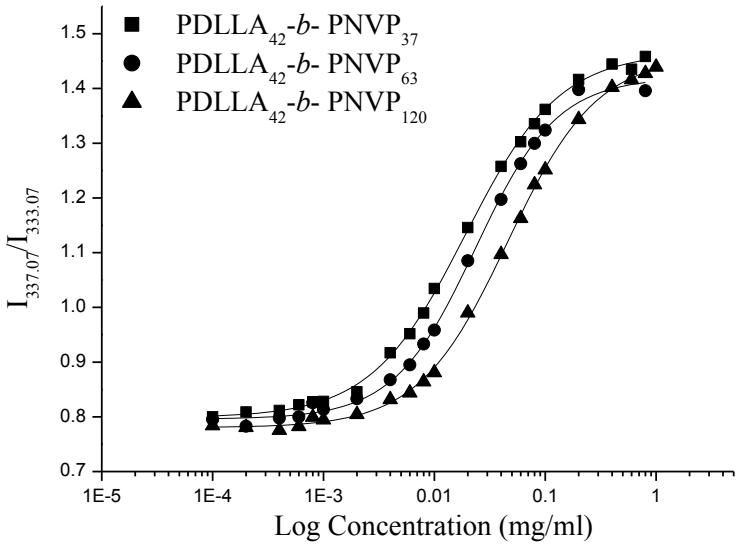

(b)

Figure 2.9(a) Fluorescence excitation spectra (monitored at λ_{em} = 394 nm) of pyrene (6 × 10^{-7} M) in the presence of increasing concentration (C) (mg/mL) of block copolymer PDLLA$_{42}$-*b*-PNVP$_{63}$ (**run 2**, **Table 2.2**) solution in water and **(b)** semilogarithmic plot of the fluorescence excitation intensity ratio ($I_{337.07}/I_{333.07}$) of pyrene (6 × 10^{-7} M) (monitored at λ_{em} = 394 nm) vs. the concentration of PDLLA$_{42}$-*b*-PNVP$_{37}$ (**run 1**), PDLLA$_{42}$-*b*-PNVP$_{63}$ (**run 2**),and PDLLA$_{42}$-*b*-PNVP$_{120}$ (**run 3**) block copolymers in water (**Table 2.2**).

pyrene (6×10^{-7} M) at different PDLLA$_{42}$-*b*-PNVP$_{63}$ concentrations recorded at an emission wavelength of 394 nm are shown in **Figure 2.9(a)**. The plots of the $I_{337.07}/I_{333.03}$ intensity ratio (from fluorescence measurements) vs. the log of the block copolymer concentration (mg/mL) in water for PDLLA$_{42}$-*b*-PNVP$_{37}$, PDLLA$_{42}$-*b*-PNVP$_{63}$, and PDLLA$_{42}$-*b*-PNVP$_{120}$, respectively, are shown in **Figure 2.9(b)**.The observed *cmc*s of these block copolymers are ~2.4×10^{-3}, ~3.4×10^{-3}, and ~6.0×10^{-3} mg/mL, respectively. The *cmc*s of the block copolymers PDLLA$_{64}$-*b*-PNVP$_{24}$, and PDLLA$_{64}$-*b*-PNVP$_{48}$, are observed at ~2.1×10^{-3}, and ~3.4×10^{-3} mg/mL, respectively (**Table 2.2**). These results indicate that the *cmc* value of block copolymer increases with the increase in the chain length of PNVP block. Similar type of results has also been reported by our group [Mishra *et al*. (2011)] for PCL-*b*-PNVP system.

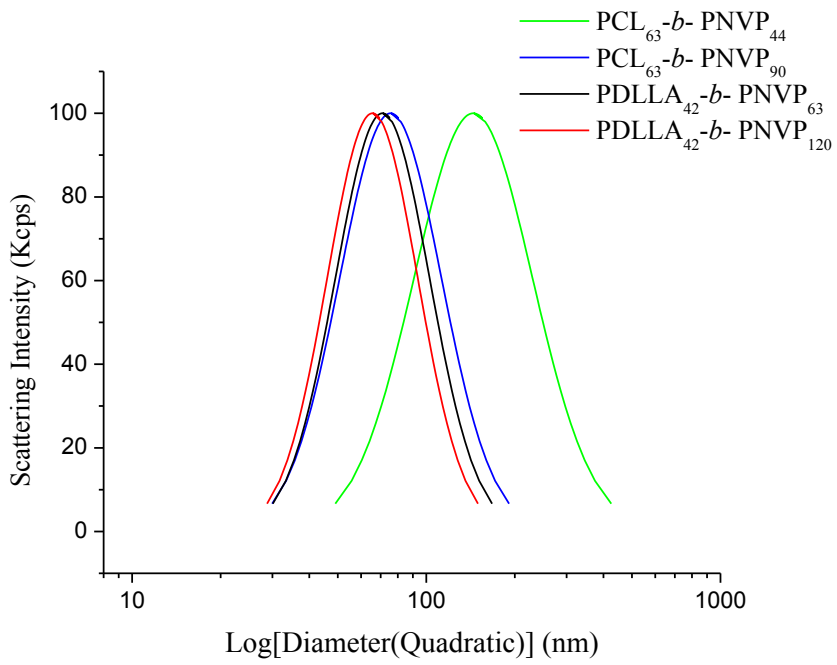

Figure 2.10 Plot of scattering intensity *vs.* effective hydrodynamic diameter (quadratic) of PCL$_{63}$-*b*-PNVP$_{44}$ at 0.09 mg/mL [Mishra *et al*. (2011)], PCL$_{63}$-*b*-PNVP$_{90}$ at 0.3 mg/mL [Mishra *et al*. (2011)], PDLLA$_{42}$-*b*-PNVP$_{63}$ and PDLLA$_{42}$-*b*-PNVP$_{120}$, at 0.5 mg/mL concentration in water at 90^{o} scattering angle.

The plot of scattering intensity vs. effective hydrodynamic diameter (quadratic) of the micelles formed at well above the corresponding *cmc* values in water at 90^{o} scattering angle for the block copolymers prepared in **runs 2** and **3** of **Table 2.2** is shown in **Figure 2.10**. Unimodal distribution curves are formed for all block copolymers, and this observation indicates the formation of relatively similar sized micellar aggregates from the corresponding block copolymers. It also clearly indicates that the hydrodynamic volume of the micelle formed from PDLLA-*b*-PNVP block copolymers in water at room temperature decreases with the increase in the chain length of hydrophilic PNVP block. We also observed similar type of observation for PCL_{63}-*b*-PNVP block copolymer systems reported earlier from our group [Mishra *et al*. (2011)], which are also included in the same figure for comparison. Such observation may be (i) due to the involvement of lesser no of block copolymer molecules having higher hydrophilic block length in forming its micelle or, (ii) due to the stronger interactions of the longer hydrophilic groups among themselves at the shell part of the micelles assuming that core part, which is made of hydrophobic block, remains unchanged or, (iii) due to both reasons as mentioned above. The observed shorter hydrodynamic volume in case of PLA system may be due to (i) its shorter PLA block length as well as due to (ii) the stronger interaction of PLA block among themselves within the core part through its two ester groups within each monomeric unit. Moreover, with the doubling of PNVP block length, the decrement of the hydrodynamic volume is considerable for PCL system. This may be (i) due to the greater compatibility of PCL and PNVP blocks having relatively similar structural units with respect to that of PDLLA and PNVP blocks, which have relatively different structural units or, (ii) due to the aggregation of sparingly soluble PCL_{63}-$PNVP_{44}$ block

copolymers in water. All these observations are as per the conclusions drawn by Sheng et al. [Sheng *et al*. (2007)] on the basis of dissipative particle dynamics for the distribution of micellar size for diblock copolymers with different soluble block lengths. Similar type of observations is also reported earlier by Forster *et al*. (1996).

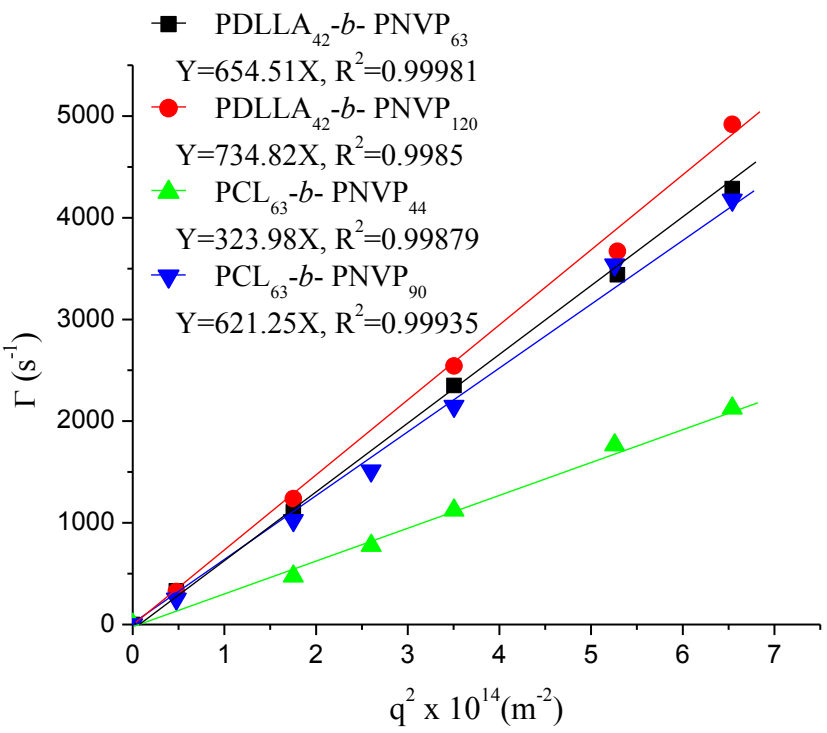

Figure 2.11 Plot of average decay rates (Γ) vs. the square of the scattering vector (q^2) of PCL_{63}-*b*-$PNVP_{44}$ at 0.09 mg/mL [Mishra *et al*. (2011)], PCL_{63}-*b*-$PNVP_{90}$ at 0.3 mg/mL [Mishra *et al*. (2011)], $PDLLA_{42}$-*b*-$PNVP_{63}$ and $PDLLA_{42}$-*b*-$PNVP_{120}$, at 0.5 mg/mL concentration in water.

The corresponding plots of average decay rates (Γ) vs. the square of the scattering vector (q^2) [**Figure 2.11**] are linear, which indicates the formation of micelles through translational diffusion. The corresponding slope (translational diffusion coefficient, D) increases with increase in the PNVP chain length as expected due to the smoother formation of micelle. Similar types of results are also reported in the literature. [Mishra *et al*. (2011), Chung *et al*. (2004)] Considerably smaller value of

D for PCL_{63}-*b*-$PNVP_{44}$ indicates relatively un-smooth formation of its micelle as expected from the explanations given in the previous paragraph.

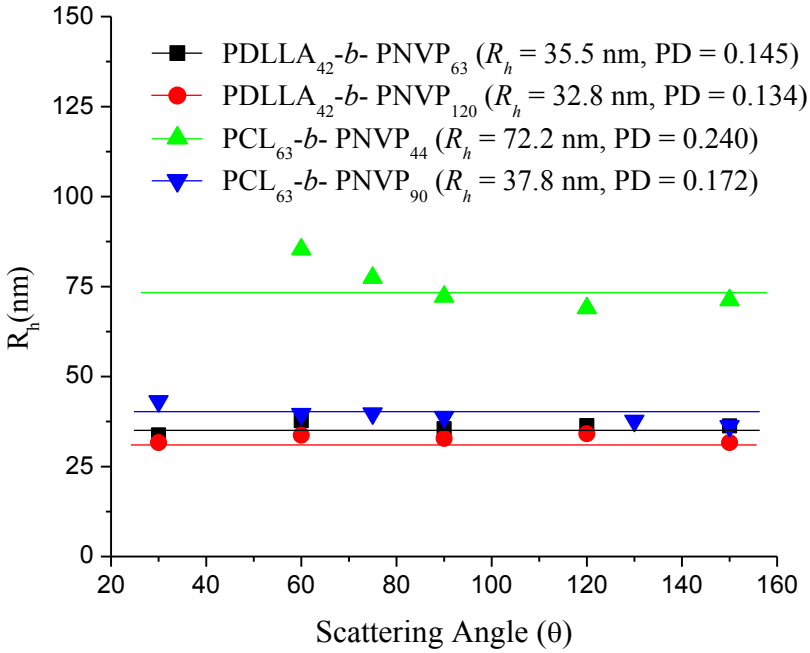

Figure 2.12 Plot of DLS measurement/scattering angles vs. the hydrodynamic radius (R_h) of the micelles of the PCL_{63}-$PNVP_{44}$ at 0.09 mg/mL [Mishra *et al*. (2011)], PCL_{63}-$PNVP_{90}$ at 0.3 mg/mL [Mishra *et al*. (2011)], $PDLLA_{42}$-*b*-$PNVP_{63}$ and $PDLLA_{42}$-*b*-$PNVP_{120}$, at 0.5 mg/mL concentration of block copolymers in water.

Figure 2.12 shows that the corresponding hydrodynamic radii (R_h) of the micelles remained almost constant under the measured range of scattering angle variation. This result clearly indicates the formation of spherical micelles for both PLA and PCL [Mishra *et al*. (2011)] systems through association mechanism. [Chu *et al*. (1991)] The deviation from linearity for PCL_{63}-*b*-$PNVP_{44}$ system at lower scattering angle indicates the possible formation of non-spherical micelle from itself.

Moreover, TEM study shows the formation of micelle with the radius of ~15.1 nm from the aqueous solution of $PDLLA_{42}$-*b*-$PNVP_{63}$ block copolymer [**Figure 2.13**].

This value is smaller than that (~35.5 nm) observed from DLS measurement. This may be due to the collapse of the micellar structure on TEM grids during drying process. Results are also in good agreement with that of PCL-*b*-PNVP block copolymer system, reported earlier from our group.[Mishra *et al*. (2011)] All these results confirm the amphiphilic character of these block copolymers.

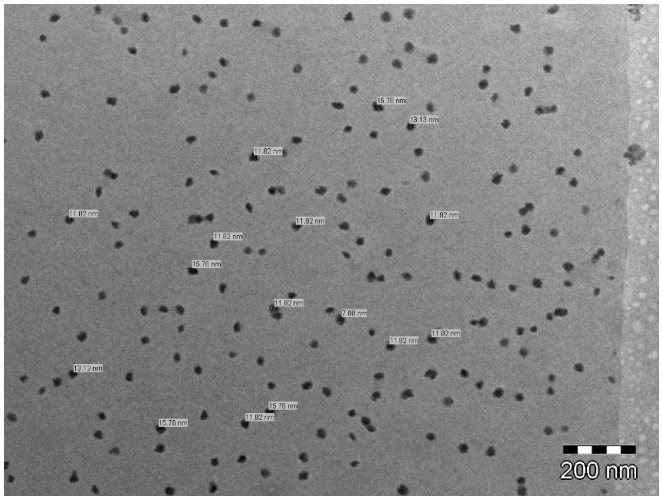

Figure 2.13 TEM image of the micelles obtained from aqueous solution (1 mg/mL) of $PDLLA_{42}$-*b*-$PNVP_{63}$ (**run 2, Table 2.2**).

2.3.4 Thermal Study

The thermal stability of the block copolymers was studied using TGA and DTA. **Figure 2.14(a)** shows the TGA curves of $PDLLA_{42}$-X, PNVP (M_n = 6000 g mol^{-1}, PDI = 1.25) homopolymer and $PDLLA_{42}$-*b*-$PNVP_{37}$ block copolymer. The decomposition of PDLLA occurs through one step degradation initiated at 316 ^oC; on the other hand, PNVP has a higher thermal stability than PDLLA-X. PNVP undergoes initial slight weight loss at ~ 90-120 ^oC owing to the evaporation of adsorbed moisture followed by broad mass loss in the region ~ 400-420 ^oC due to the degradation of the backbone chain of PNVP. [Bartels *et al*. (2009)] $PDLLA_{42}$-*b*-$PNVP_{37}$ block copolymer has two

steps degradation initiated at ~ 298ºC and ~ 401 ºC due to PDLLA block, and PNVP block, respectively, suggesting the presence of two different blocks in the polymer.

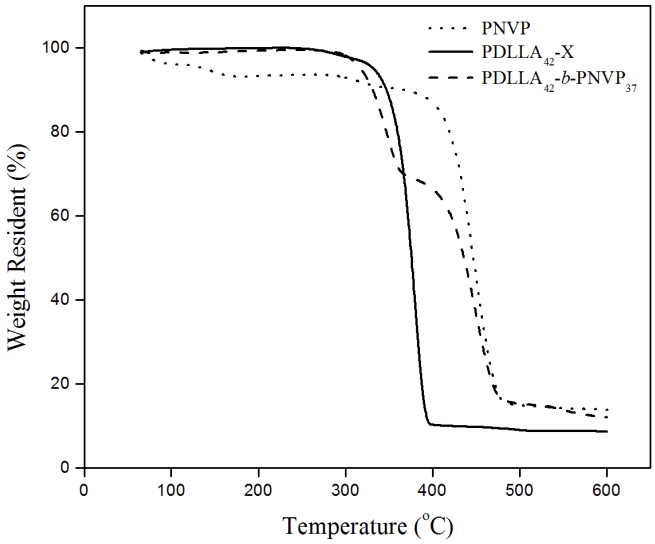

(a)

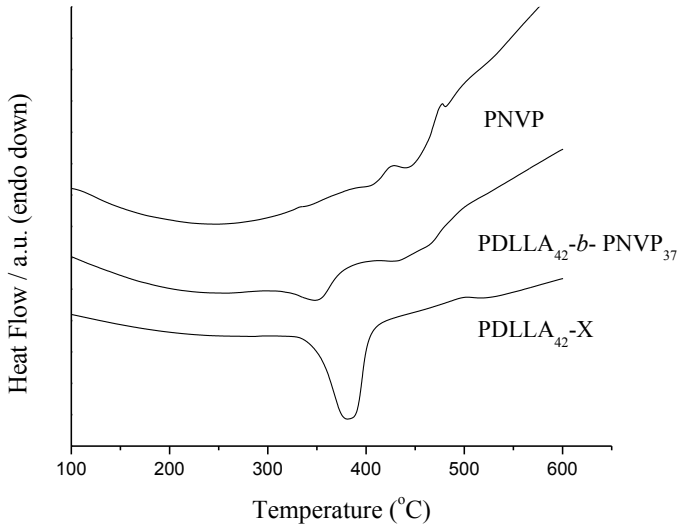

(b)

Figure 2.14(a) TGA and **(b)** DTA thermograms of $PDLLA_{42}$-X, PNVP, and $PDLLA_{42}$-*b*-$PNVP_{37}$ block copolymer. Heating rate: 20 °C/min under N_2.

These data are supported by DTA thermograms in **Figure 2.14(b**), where two endothermic peaks for block copolymer are due to the degradation of two individual blocks in contrast to two separate peaks observed for homopolymers. Double endothermic peak for pure PNVP is presumably due to the degradation of the pendant group and the main chain and the corresponding degradation in block copolymer becomes wide in nature.

DSC thermograms of the $PDLLA_{42}$-X, PNVP (M_n = 6000 g mol^{-1}, PDI = 1.25) homopolymers and two block copolymers $PDLLA_{42}$-*b*-$PNVP_{37}$ and $PDLLA_{42}$-*b*-$PNVP_{63}$ are shown in **Figure 2.15**. In second heating runs, the glass transition temperature (T_g) of $PDLLA_{42}$-X is observed at ~ 41 ^oC. PNVP did not show any melting endotherm or exotherm. [Ansari *et al*. (2008)] The secondary transition temperature at 100 ^oC is due to the relaxation of its pendent pyrrolidone group. The sharp secondary transition temperature at 155 ^oC is due to the glass transition temperature (T_g) of the backbone chain of PNVP. The single glass transition temperatures (T_g) of $PDLLA_{42}$-*b*-$PNVP_{37}$ and $PDLLA_{42}$-*b*-$PNVP_{63}$ are observed at ~ 115 and 122 ^oC, respectively. This observation of the single T_g peak of the block copolymers may be due to the miscibility of the PDLLA segment with the amorphous PNVP.

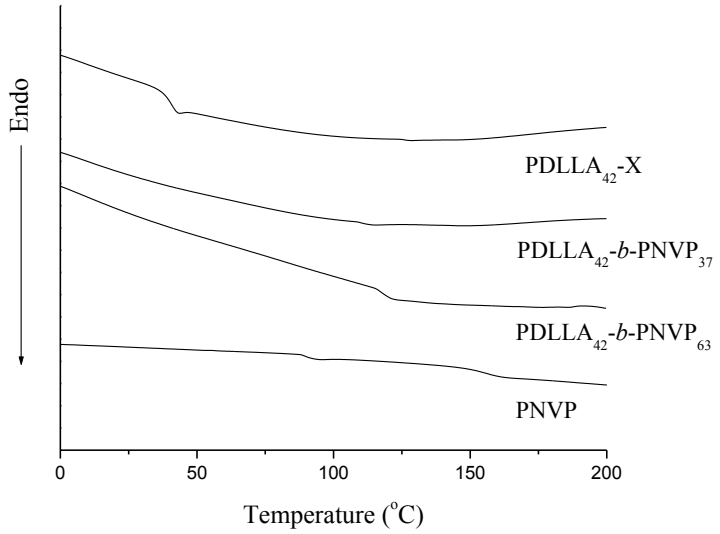

Figure 2.15 DSC thermograms of $PDLLA_{42}$-X and PNVP homopolymers, and $PDLLA_{42}$-*b*-$PNVP_{37}$ and $PDLLA_{42}$-*b*-$PNVP_{63}$ block copolymers. Heating rate: 10 °C/min under N_2.

2.3.5 XRD Study

XRD results of the $PDLLA_{42}$-X homopolymer, and two block copolymers $PDLLA_{42}$-*b*-$PNVP_{63}$, and $PDLLA_{42}$-*b*-$PNVP_{120}$ are shown in **Figure 2.16**. $PDLLA_{42}$-X shows the intense characteristic diffraction peaks located at 2θ = 13.8, and 16.7°. [Letizia *et al*. (2002)] The $PDLLA_{42}$-*b*-$PNVP_{63}$ and $PDLLA_{42}$-*b*-$PNVP_{120}$ block copolymers also have the same characteristic peaks with low intensity confirming the presence of amorphous PNVP macro-domain in block copolymer. It is presumed that PDLLA macro-domain and PNVP macro-domain interact with each other at the molecular level indicating certain miscibility and support the single glass transition temperature observed in DSC studies.

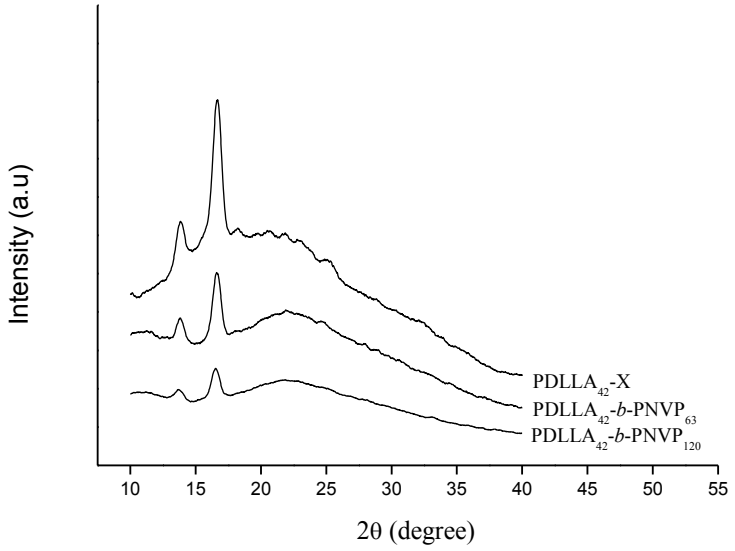

Figure 2.16 XRD of $PDLLA_{42}$-X homopolymer, $PDLLA_{42}$-*b*-$PNVP_{63}$ and $PDLLA_{42}$-*b*-$PNVP_{120}$ block copolymers.

Therefore, all these results support the successful formation of block copolymer of PDLLA and PNVP and confirmed the amphiphilic character of these two block copolymers.

2.3.6 MTX Loading and *In Vitro* Release Study

Methotrexate (MTX) is a poorly water-soluble anticancer drug. It can easily be encapsulated into the hydrophobic core part of the polymeric micelle *via* hydrophobic interaction. The MTX-loaded $PDLLA_{42}$-*b*-$PNVP_{63}$ micelles were prepared by using dialysis method. The amount of MTX encapsulated into polymeric micelle was calculated from absorbance of MTX at 308 nm from UV measurement on comparison with a calibration curve [**Figure 2.17**].

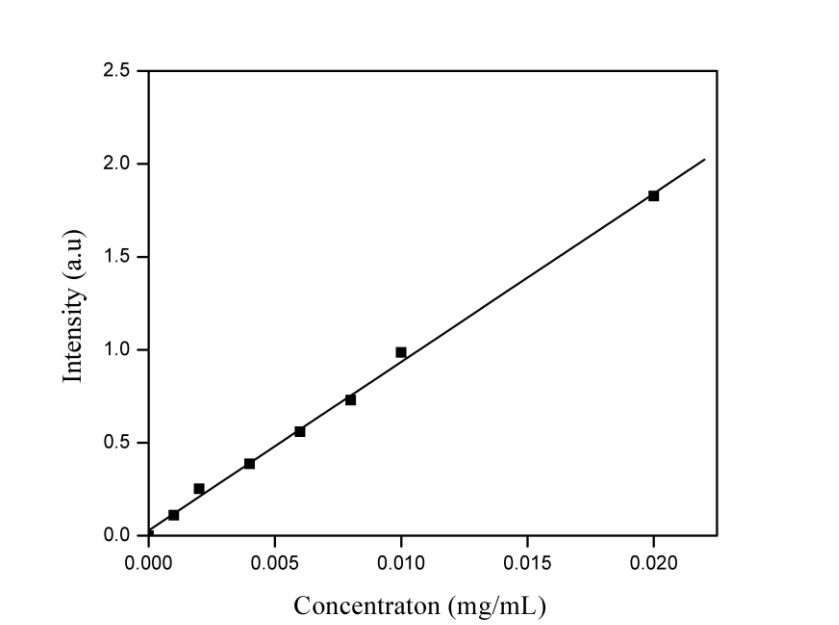

Figure 2.17 The calibration curve of Methotrexate drug in DMF solutions.

$PDLLA_{42}$-*b*-$PNVP_{63}$ micelles were successfully loaded with MTX with drug loading content of 6.5 % and drug loading efficiency of 27%. TEM study clearly shows the larger micellar size for drug-loaded micelle (98 nm dia) [**Figure 2.18**] with respect to its unloaded micelle (30.2 nm dia) as expected [**Figure 2.13**].

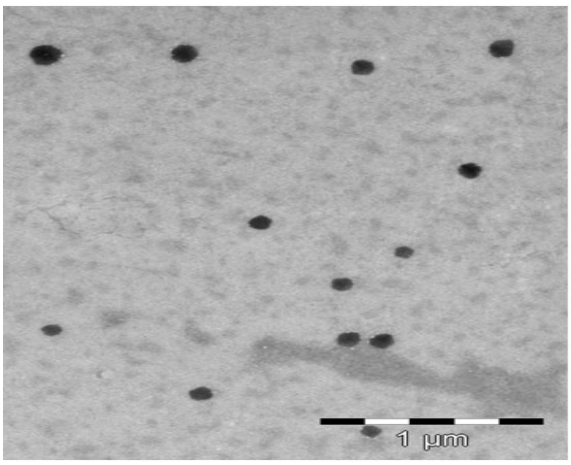

Figure 2.18 The TEM image of MTX drug loaded micelles of linear $PDLLA_{42}$-*b*-$PNVP_{63}$

DLS study shows the larger (266.8 nm with PDI = 0.578) hydrodynamic diameter of the MTX drug-loaded micelle of PDLLA$_{42}$-*b*-PNVP$_{63}$ with respect to that of the parent micelle (83.3 nm with PDI = 0.263) [**Figure 2.19**].

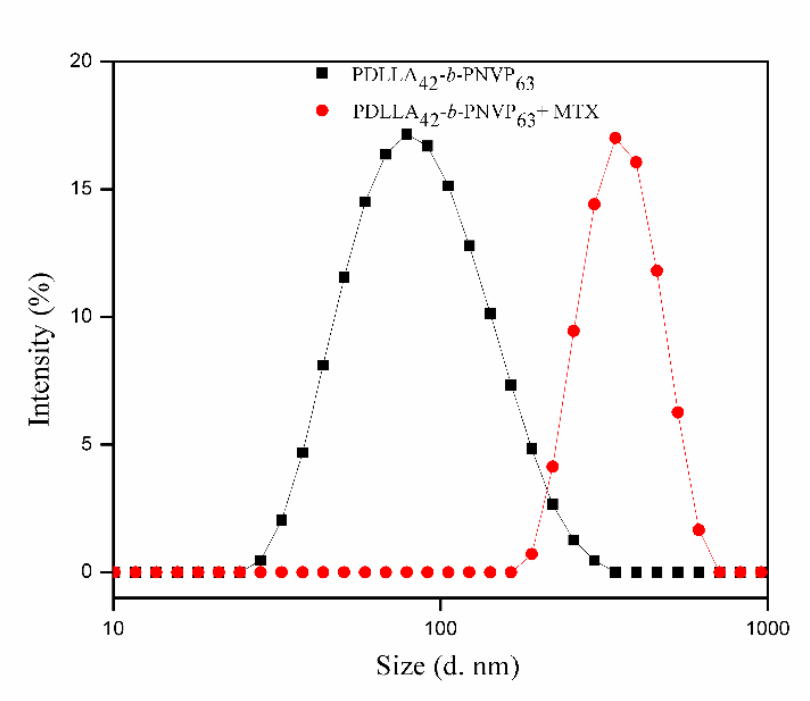

Figure 2.19 Plot of scattering intensity vs. the effective hydrodynamic diameter of MTX loaded and blank micelles of PDLLA$_{42}$-b-PNVP$_{63}$ block copolymer at 0.5 mg/mL concentration in water at 90° scattering angle.

The *in vitro* drug release study was carried out at 37 ^{o}C in pH = 6.4 and 7.4 PBS solutions. MTX loaded micelles show considerably continued release behaviors up to 43.5 and 24.8% during initial 12 h [**Figure 2.20**]. Slow drug release is very important for drug delivery, so that polymeric carriers can deliver drug to the targeted tissue after long time circulation through the bloodstream.

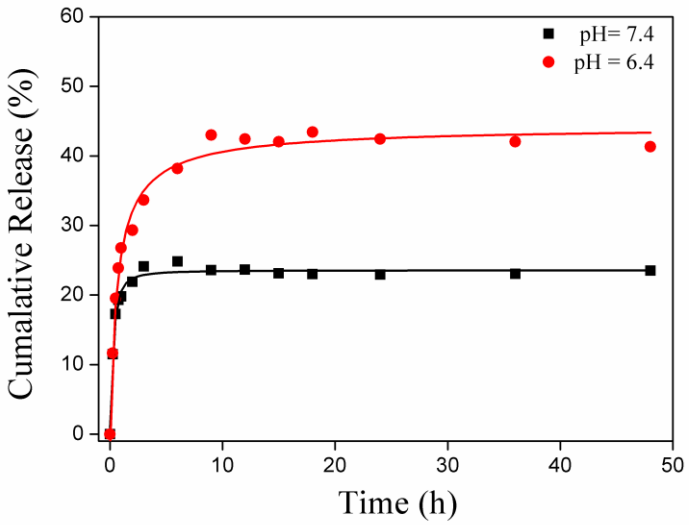

Figure 2.20 Percentage of cumulative release of MTX from PDLLA$_{42}$-*b*-PNVP$_{63}$ micelles in pH 6.4 and 7.4 PBS solutions at 37 ^{o}C temperature.

In vitro drug release behavior of polymeric micelles is also dependent on the chemical composition of polymeric micelles. The observed slow drug release is probably due to strong interaction between hydrophobic MTX drug and hydrophobic PDLLA at core. This result is comparable with previous literature reports. [Wei *et al*. (2007), Zhang *et al*. (2005)]

2.3.7 Effect of MTX-loaded PDLLA$_{42}$-*b*-PNVP$_{63}$ on Tumor Cell Viability and Cytotoxicity

We performed cell viability and cellular cytotoxicity study by the MTX-loaded PDLLA$_{42}$-*b*-PNVP$_{63}$ amphiphilic block copolymer micelles against parental and MTX-resistant human (Raji) and mouse lymphoma cells (DL) [**Figure 2.21**]. Compared to

free MTX, MTX-loaded PDLLA$_{42}$-*b*-PNVP$_{63}$ micelles significantly inhibit the cell viability in a concentration dependent manner against the cells tested.

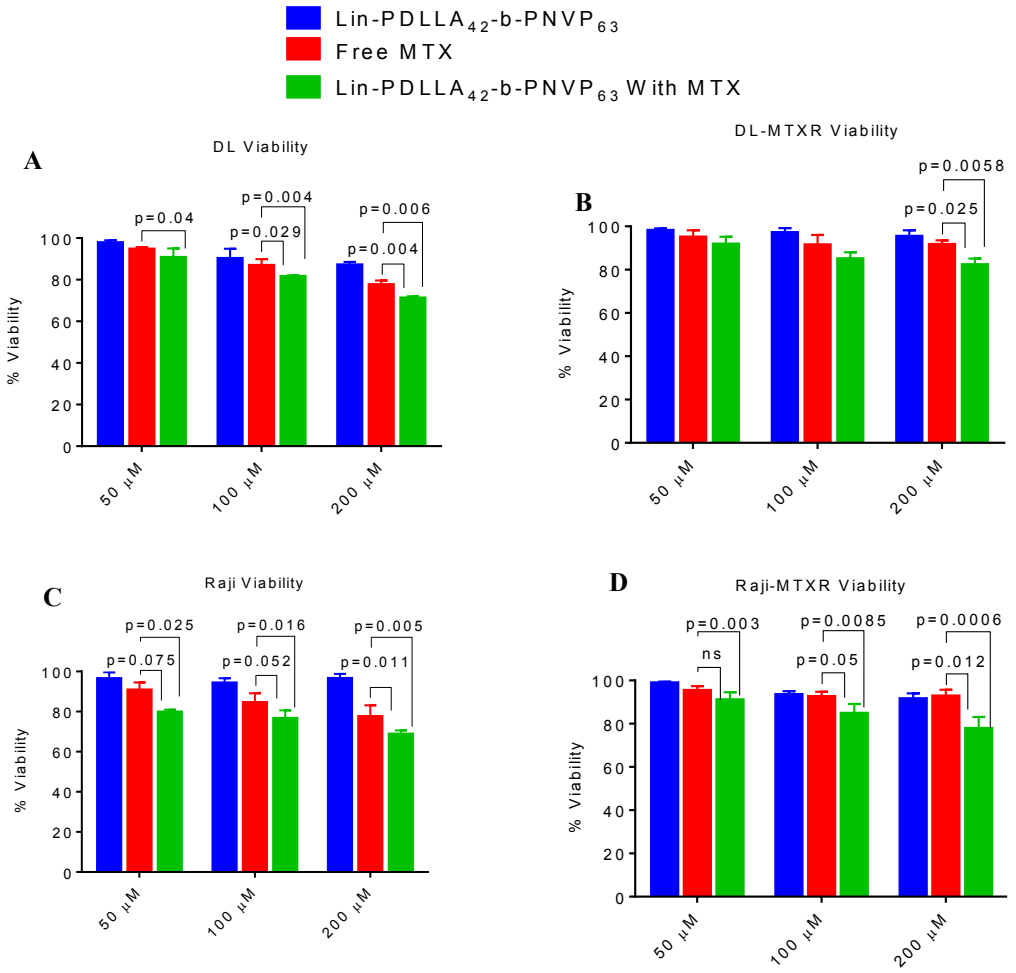

Figure 2.21 Enhanced killing of tumor cells by free MTX, PDLLA$_{42}$-*b*-PNVP$_{63}$ and MTX-loaded PDLLA$_{42}$-*b*-PNVP$_{63}$ micelles.(**A, B**) Viability of parental DL and Raji and (**C, D**) MTX resistant DL and Raji cells were studied by XTT viability assay. Data presented as mean ± SD of triplicate determination, n = 4 where n represents the number of times experiment was performed.

Parental DL (A) and Raji (C) responded better with significantly higher loss of cell viability in the presence of MTX-loaded PDLLA$_{42}$-*b*-PNVP$_{63}$ micelles compared to MTX alone [**Figure 2.21 (A)** and **(C)**]. On the other hand, the resistant DL or, Raji cells are tolerant to MTX but remain sensitive to MTX-loaded

PDLLA$_{42}$-*b*-PNVP$_{63}$ micelles [**Figure 2.21 (B)** and **(D)**]. Carrier it-self has no effect on cell viability in any of the cell line tested.

Stimuli (pH, temperature etc.) sensitive biodegradable polymers have recently been developed with faster intracellular drug release feature in tumor cells and ability to reverse multidrug resistance (MDR) in cancer cells. [Sun *et al*. (2010), Torchilin *et al*. (2011)] Our data show that MTX-loaded PDLLA$_{42}$-*b*-PNVP$_{63}$ micelles works well in lower pH compared to higher pH suggesting its better suitability in acidic environment inside the tumor cells. This was supported by the susceptibility of human and murine lymphoma cells against MTX-loaded PDLLA$_{42}$-*b*-PNVP$_{63}$ micelles with respect to cellular cytotoxicity [**Figure 2.22 (A) to (D)**]. The results suggest that MTX-loaded PDLLA$_{42}$-*b*-PNVP$_{63}$ micelles are highly cytotoxic compared to free MTX at each molar concentration tested [**Figure 2.22 (A)** and **(C)**]. The carrier it-self do not show cytotoxicity against any of the cell lines tested. Resistant variants of DL and Raji are tolerant to free MTX but remain susceptible to cytotoxicity by MTX-loaded PDLLA$_{42}$-*b*-PNVP$_{63}$ micelles at all the concentrations tested [**Figure 2.22 (B)** and **(D)**].

2.3.8 Cellular Growth Inhibition by MTX-loaded PDLLA$_{42}$-*b*-PNVP$_{63}$ Micelles

The cell viability and cytotoxicity data suggests that MTX-loaded PDLLA$_{42}$-*b*-PNVP$_{63}$ micelles have significantly higher anti-tumor potential with respect to the reduction in the viability of lymphoma cells of human and mouse origin. The development of multidrug resistance (MDR) has been a major impediment to the success of cancer chemotherapy due to its requirement for high dose regimens accompanied with increased toxicity and need for specific drug release rates during disease evolution.

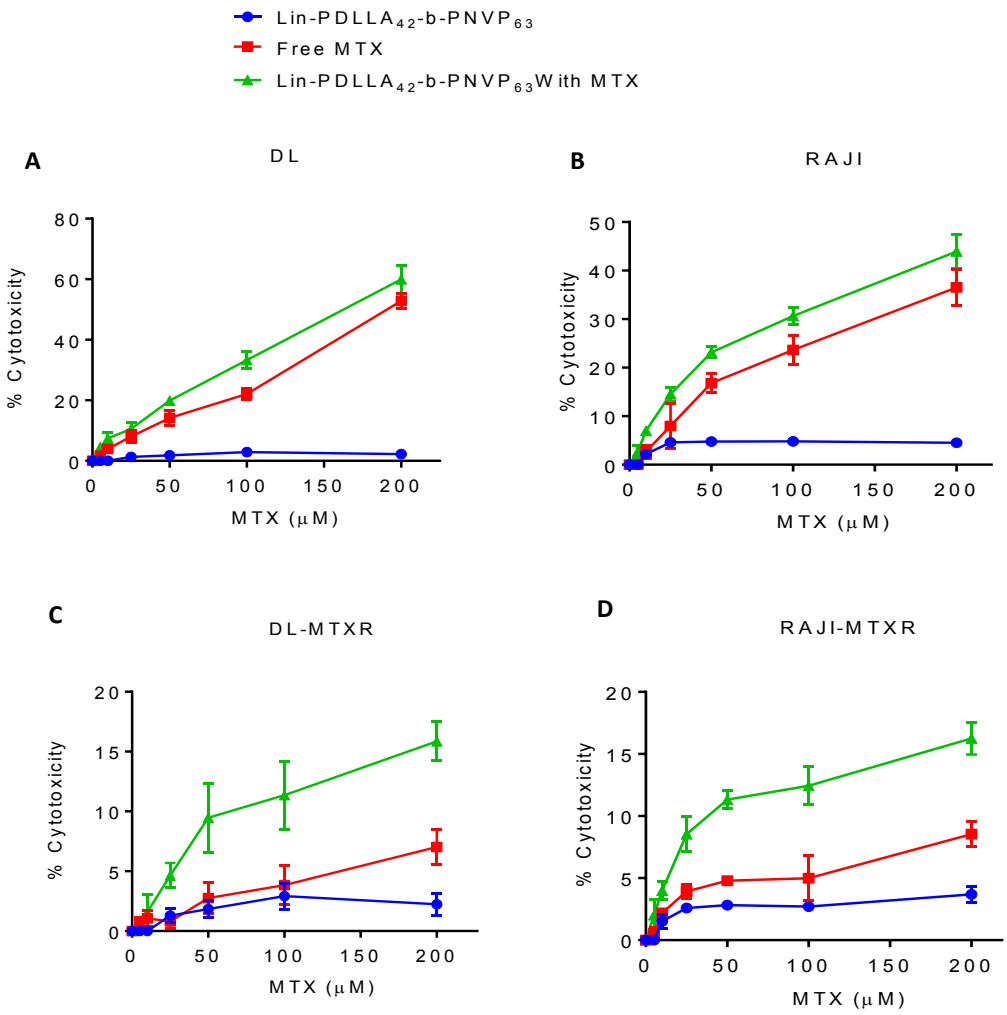

Figure 2.22 The cytotoxicity of free MTX, PDLLA$_{42}$-*b*-PNVP$_{63}$ and MTX-loaded PDLLA$_{42}$-*b*-PNVP$_{63}$ against parental or, MTX resistant DL (**A**, **B**) or, Raji cells (**C, D**) were determined by LDH release assay. Data presented as mean ± SD of triplicate determination, n = 4 where n represents the number of times experiment was performed.

Our formulation of MTX-loaded PDLLA$_{42}$-*b*-PNVP$_{63}$ micelles showed significant growth inhibition against resistant variants of human and mice lymphoma cells, suggesting broad spectrum usefulness of the compound [**Figure 2.23 (A) to (D)**]. Growth inhibition with MTX-loaded PDLLA$_{42}$-*b*-PNVP$_{63}$ micelles was significantly higher compared to its free MTX. IC$_{50}$ for MTX-resistant DL increases to 460 and 174

μM from 174 and 74 µM, respectively, from their MTX sensitive counterpart [**Figure 2.23 (A)** and **(B)**]. Similar results were also observed in MTX resistant Raji [**Figure 2.23 (C)** and **(D)**].

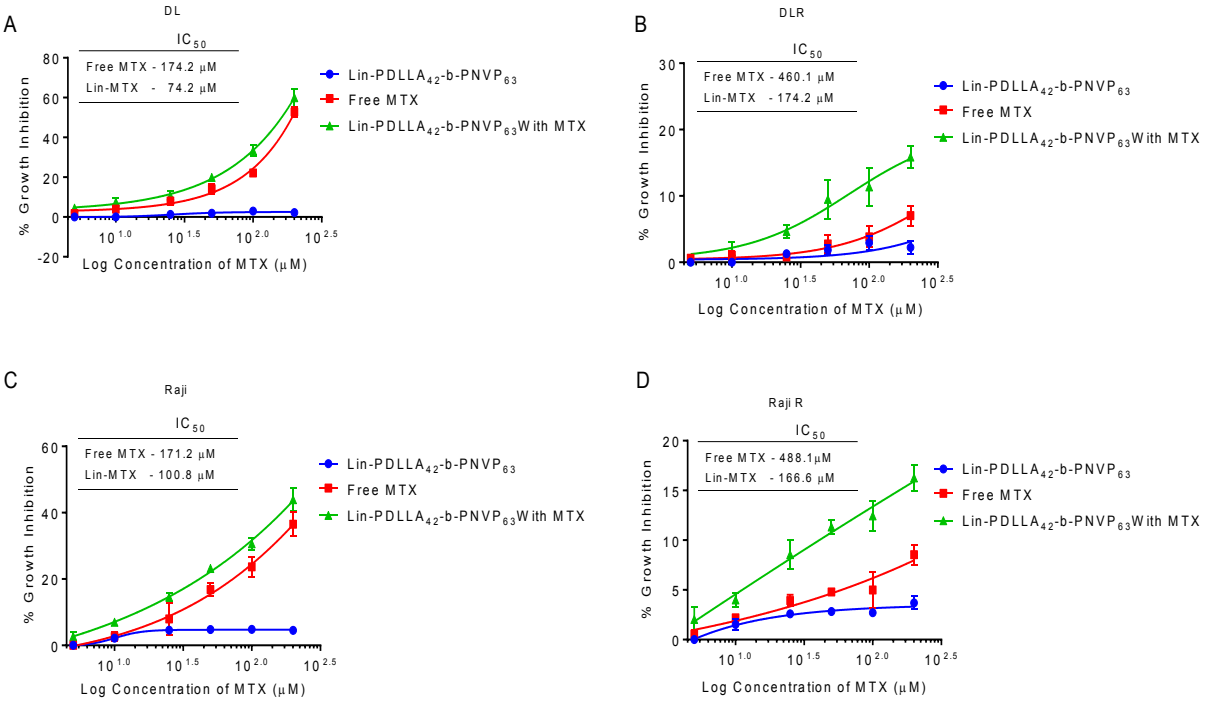

Figure 2.23. PDLLA$_{42}$-*b*-PNVP$_{63}$ retards growth of MTX resistant B cell lymphoma. Graphs show MTX concentration response on cell proliferation and growth after treatment with free MTX and PDLLA$_{42}$-*b*-PNVP$_{63}$ micelles in parental and MTX resistant DL (**A** and **B**) or, (**C** and **D**) Burkitt lymphoma cell line Raji. Data presented as mean ± SD, n = 5. Differences in IC50 values between parental and MTX resistant cell lines are mentioned.

2.3.9 Induction of Tumor Cell Apoptosis by MTX-loaded PDLLA$_{42}$-*b*-PNVP$_{63}$ Micelles

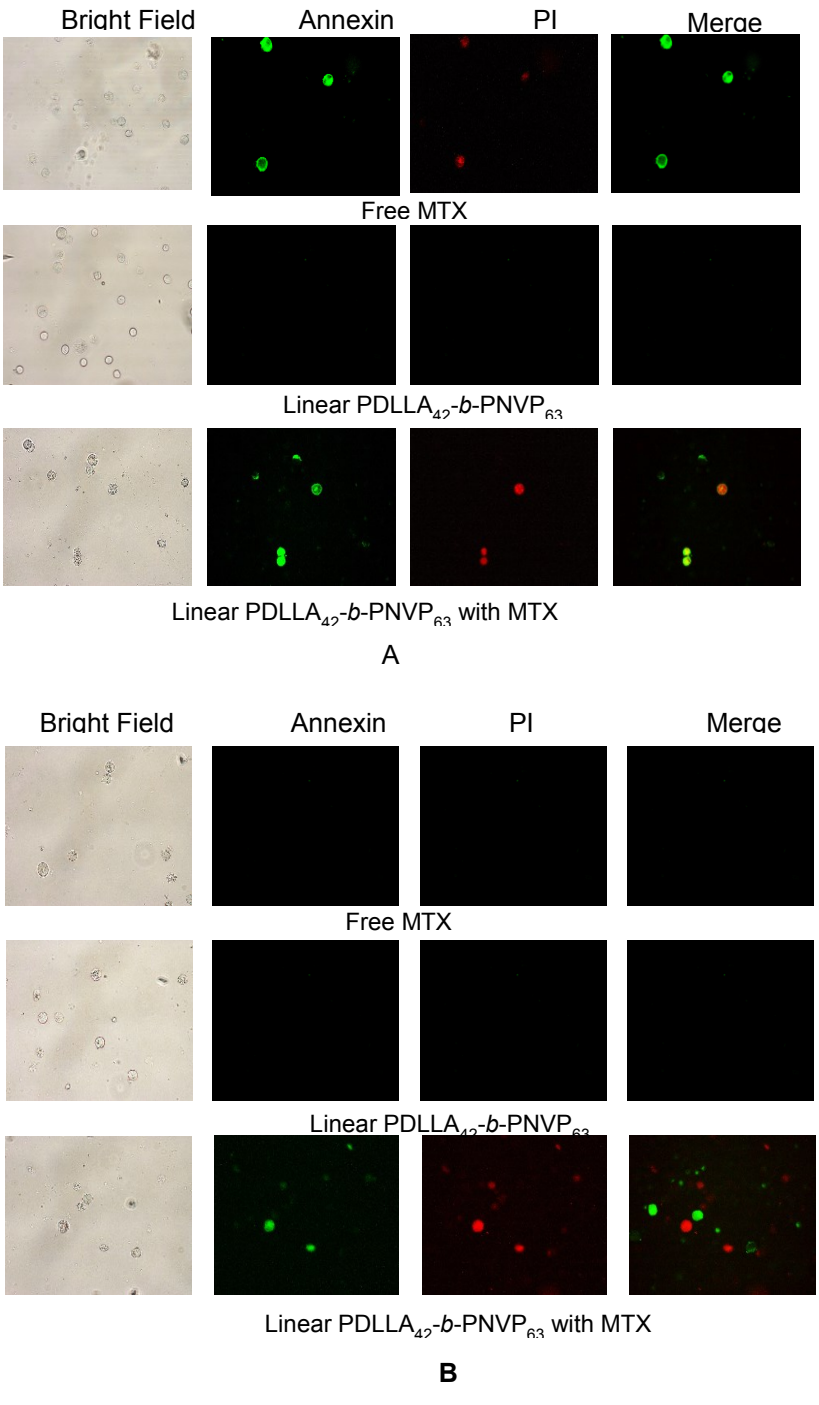

Figure 2.24 Microscopic analysis of induction of apoptosis in DL. Parental DL (**A**) and MTX-R/DL (**B**) Cells were treated with free MTX, free polymer and MTX loaded PDLLA$_{42}$-*b*-PNVP$_{63}$ micelles with equivalent MTX at a concentration of 5.0 μM. n=4.

Broad spectrum growth inhibition by MTX-loaded PDLLA$_{42}$-*b*-PNVP$_{63}$ micelles raises the question whether it also causes apoptosis of tumor cells and if so whether it induces cell death in MTX-resistant tumor cells, which become refractory to any concentrations of MTX. Apoptosis was determined by monitoring changes in cell size and externalization of phosphatidylserine qualitatively in parental and MTX resistant DL to document the events of apoptosis. There was an abundance of Annexin V positive cells in parental DL treated linear PDLLA$_{42}$-*b*-PNVP$_{63}$ amphiphilic block copolymers which are significantly higher compared to free MTX treatment. Resistant variants of the DL exhibits tolerance to free MTX but become susceptible to MTX-loaded PDLLA$_{42}$-*b*-PNVP$_{63}$ micelles. [**Figure 2.24 (A)** and **(B)**]

2.3.10 RBC Integrity and Size Distribution

The MTX-loaded PDLLA$_{42}$-*b*-PNVP$_{63}$ micelles did not affect RBC with respect to hemolysis. As a confirmation to RBC counting, hemolysis rate was determined in the presence of the formulations, which did not exceed the negative control value by more than 2% and, so that the MTX-loaded PDLLA$_{42}$-*b*-PNVP$_{63}$ micelles may be considered as non-hemolytic [**Figure 2.25**]. Hemolysis study at increasing time point and concentration suggests that MTX-loaded PDLLA$_{42}$-*b*-PNVP$_{63}$ micelles do not causes hemolysis compared to free MTX which is significantly hemolytic [**Figure 2.25(A)** and **(B)**]. Microscopic observations also demonstrate no change in morphology of RBC following contact with the MTX-loaded PDLLA$_{42}$-*b*-PNVP$_{63}$ micelles [**Figure 2.25 (C)**]. Free MTX, on the other hand, is hemolytic at all the concentrations tested. Thus, we may conclude that the MTX-loaded PDLLA$_{42}$-*b*-PNVP$_{63}$ micellar formulation is inert toward the blood's major cellular component.

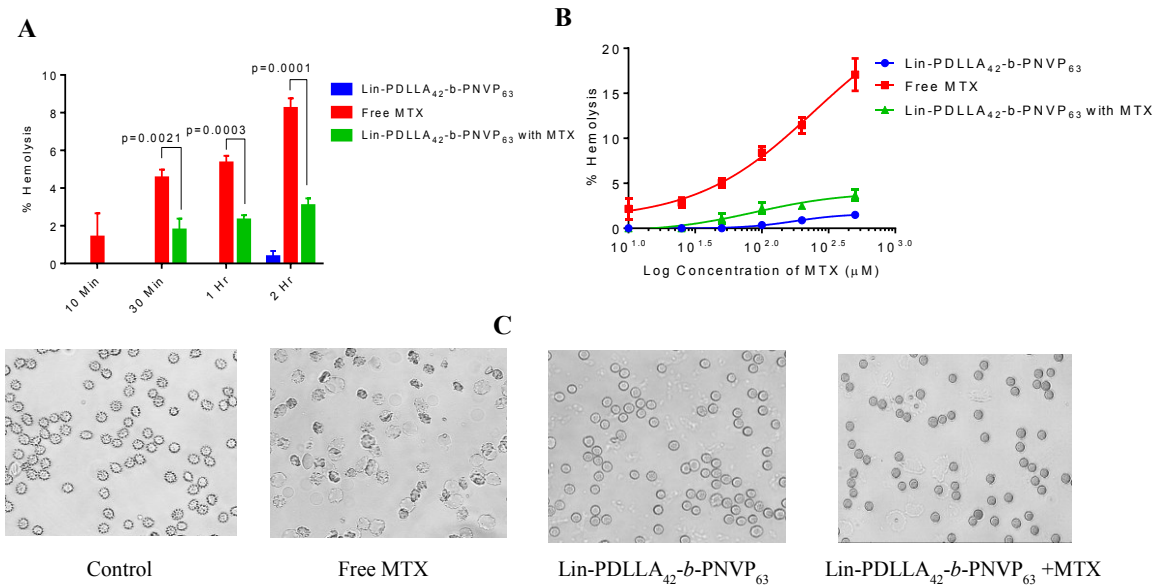

Figure 2.25 Hemolytic assay. Hemolysis induced by MTX and MTX-loaded PDLLA$_{42}$-*b*-PNVP$_{63}$ micelles in whole human blood for a (**A**) fixed concentration or, (**B**) increasing concentrations and is expressed as percent whole blood hemoglobin content. Mean ± SD, n = 3. (**C**) Photomicrographs demonstrate the absence of action of MTX-loaded PDLLA$_{42}$-*b*-PNVP$_{63}$ micelles on RBC morphology in comparison to MTX treatment alone.

2.3.11 MTX-loaded PDLLA$_{42}$-*b*-PNVP$_{63}$ Micelles Tolerant to Normal Cell Viability and Cytotoxicity

Unlike tumor cells, white blood cells from normal human peripheral blood mononuclear cell (PBMC) show tolerance to MTX-loaded PDLLA$_{42}$-*b*-PNVP$_{63}$ micelles [**Figure 2.26**]. Viability of PBMC and cellular fractions like dendritic cells (DC) remain unaltered in the presence of MTX-loaded polymer micelles [**Figure 2.26 (A)** and **(B)**]. In contrast, free MTX causes reduction in cell viability of PBMC, and DC compared to MTX-loaded PDLLA$_{42}$-*b*-PNVP$_{63}$ micelles at comparable molar concentrations of MTX tested (% viability of lymphocytes 60.87 vs. 93.26 at 1 mM of

concentration, $p < 0.0001$) [**Figure 2.26 (A)** and **(B)**]. We also checked the direct cytotoxicity of MTX-loaded PDLLA$_{42}$-*b*-PNVP$_{63}$ micelles on normal cells and compared with free MTX treatment. Significantly higher cytotoxicity was observed in PBMC or, DC upon treatment with free MTX compared to MTX-loaded PDLLA$_{42}$-*b*-PNVP$_{63}$ micelles at molar concentration tested **[Figure 2.26 (C)** and **(D)**].

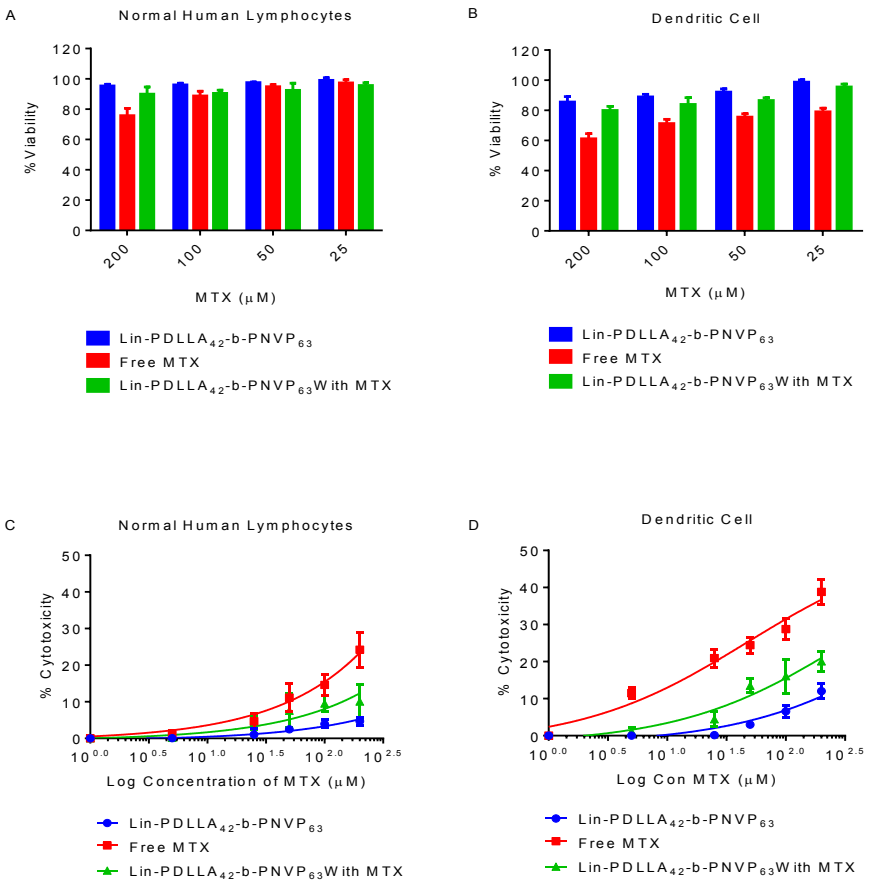

Figure 2.26 MTX-loaded PDLLA$_{42}$-*b*-PNVP$_{63}$ micelles are non-toxic to lymphocytes. Effect of free MTX and MTX-loaded PDLLA$_{42}$-*b*-PNVP$_{63}$ micelles on normal cell viability. Normal human lymphocytes (**A**), and (**B**) DC were treated with serial concentrations of MTX (0.0001, 0.005, 0.01, 0.05, 0.1, 0.5, 1, and 5 mM). The cell viability was measured by XTT assay. Data shown as mean ± SD, n = 3. Effects on leukocytes cytotoxicity was determined by 18 h LDH release assay (**C**) and (**D**). Data presented as mean ± SD of triplicate determination, n = 4.

These results suggest that normal immune cells are safe in the presence of MTX-loaded $PDLLA_{42}$-*b*-$PNVP_{63}$ micelles while free MTX significantly harms its potential. Tolerance exhibited by DC to MTX-loaded polymeric micelles compared to free MTX is significant with reference to the preservation of intact immune response mediated by DC, required for effective therapeutic response *in vivo* [**Figure 2.26(D)**].

2.4 Conclusions

Well-defined, amphiphilic, biodegradable and biocompatible linear diblock copolymers of DLLA and NVP have successfully been synthesized *via* the combination of ROP and xanthate-mediated RAFT polymerization, respectively. The resultant polymers were characterized by ^{1}H NMR, GPC, TGDTA and DSC studies, confirming successful formation of block copolymer. Formation of spherical micelles from self-assembly of these block copolymers in water is revealed by TEM study, and supported by ^{1}H NMR and light scattering studies. The *cmc* values of these block copolymers are increased with the increase in the chain length of the PNVP segment. The effective hydrodynamic volume (R_h) of the micelles above the corresponding *cmc* value is remained almost constant over the angles of scattering measurements. The TGA and DTA thermograms show two steps degradation of block copolymer started at ~ 298ºC and ~ 401 ºC, suggesting the presence of two blocks. The DSC thermograms show the presence of single glass transition temperature due to good miscibility of PNVP and PDLLA blocks. XRD study of block copolymer shows the suppression of crystalline nature of PDLLA due to the incorporation of PNVP block. Thus, all these results confirm the successful formation of well-defined PDLLA-*b*-PNVP block copolymers. The hydrophobic anticancer drug MTX has successfully been loaded inside core of

nanosized spherical micelles with drug loading content of 6.5 % and drug loading efficiency of 27%. The diameter of loaded micelles increase to 98 nm compared to 30.2 nm diameter of unloaded micelles as revealed from TEM study and also supported by DLS study. *In vitro* drug release study at pHs of 6.4 and 7.4 showed slow drug release up to of maximum 43.5 and 24.8 % reached at 12 h, probably due to strong interaction between hydrophobic MTX drug and hydrophobic PDLLA core of the micelles. The MTX-loaded micelles show significant growth inhibition, cytotoxicity, and apoptosis of DL and Raji cells compare to Free MTX. Moreover, MTX-loaded $PDLLA_{42}$-*b*-$PNVP_{63}$ micelles also suppress MTX resistant lymphoma cells while free MTX remain ineffective. In addition, MTX-loaded $PDLLA_{42}$-*b*-$PNVP_{63}$ micelles do not cause hemolysis compared to free MTX which is toxic for RBC.